City of Morro Bay and
Cayucos Sanitary District

OFFSHORE MONITORING AND REPORTING PROGRAM

FOURTH QUARTER RECEIVING–WATER SURVEY

OCTOBER 2017

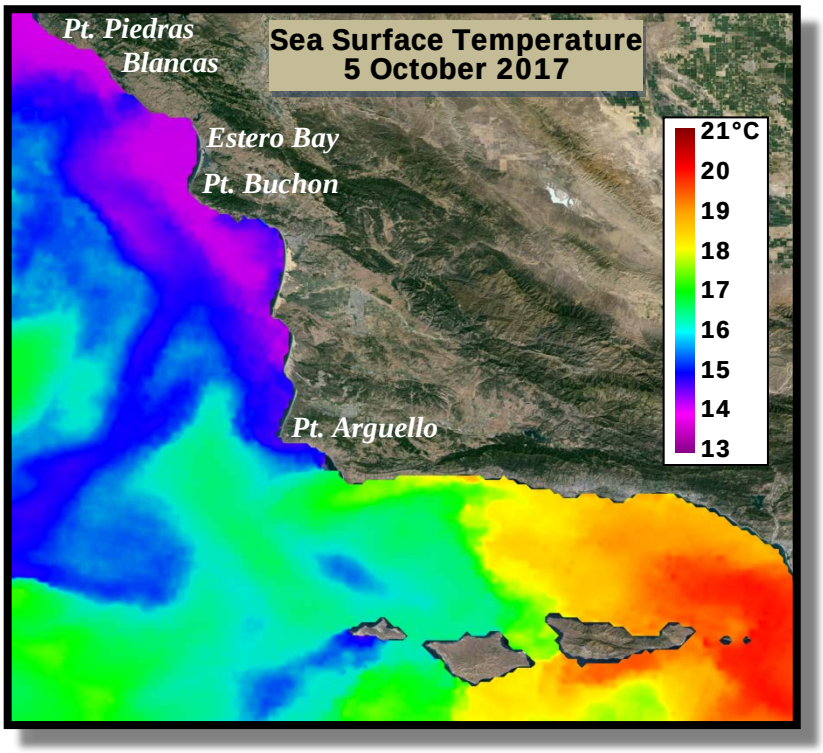

Marine Research Specialists
4744 Telephone Rd Ste 3 PMB 315
Ventura, California 93003

Report to the

City of Morro Bay and
Cayucos Sanitary District

955 Shasta Avenue
Morro Bay, California 93442
(805) 772-6272

OFFSHORE MONITORING AND REPORTING PROGRAM

FOURTH QUARTER RECEIVING–WATER SURVEY

OCTOBER 2017

Prepared by

Douglas A. Coats

Marine Research Specialists

4744 Telephone Rd Ste 3 PMB 315
Ventura, California 93003

Telephone: (805) 644-1180
E-mail: Marine@Rain.org

December 2017

marine research specialists
4744 Telephone Rd., STE 3 PMB 315 • Ventura, CA 93003 • 805-644-1180

John Gunderlock
Wastewater & Collection Systems Supervisor
City of Morro Bay
955 Shasta Avenue
Morro Bay, CA 93442

27 December 2017

Reference: Fourth Quarter Receiving-Water Survey Report – October 2017

Dear Mr. Gunderlock:

The attached report presents results from a quarterly receiving-water survey conducted on Tuesday, 10 October 2017. The survey was conducted in accordance with the requirements of the NPDES permit issued to the City and District for discharge of treated wastewater to Estero Bay. The report evaluated compliance with permit limitations and assessed the effectiveness of effluent dispersion within receiving waters. Quantitative analyses of continuous instrumental measurements and qualitative visual observations confirmed that the wastewater discharge complied with the receiving-water limitations specified in the permit, and with the objectives of the California Ocean Plan.

The offshore measurements confirmed that the diffuser structure and treatment plant continued to operate at a high level of performance. The measurements delineated a diffuse discharge plume containing low organic loads within a localized region surrounding the discharge point. Dilution within the plume exceeded expectations based on modeling and outfall design criteria.

Contact the undersigned if you have questions regarding the attached report.

Sincerely,

Douglas A. Coats

Douglas A. Coats
Program Manager

I certify under penalty of law that this document and all attachments were prepared under my direction or supervision in accordance with a system designed to assure that qualified personnel properly gather and evaluate the information submitted. Based on my inquiry of the person or persons who manage the system, or those persons directly responsible for gathering the information, the information submitted is, to the best of my knowledge and belief, true, accurate and complete. I am aware that there are significant penalties for submitting false information, including the possibility of fine and imprisonment for knowing violations.

Mr. John Gunderlock
Wastewater/Collections System Supervisor
City of Morro Bay/Cayucos CSD Wastewater Treatment Plant

Date: 12/27/17

TABLE OF CONTENTS

LIST OF FIGURES

LIST OF TABLES

INTRODUCTION

The City of Morro Bay and the Cayucos Sanitary District (MBCSD) jointly own the wastewater treatment plant (WWTP) operated by the City of Morro Bay. In March 1985, Region IX of the U.S. Environmental Protection Agency (USEPA) and the Central Coast California Regional Water Quality Control Board (RWQCB) issued the first National Pollutant Discharge Elimination System (NPDES) permit to the MBCSD. The permit incorporated partially modified secondary treatment requirements for the plant's ocean discharge. The permit has been re-issued three times, in March 1993 (RWQCB-USEPA 1993ab), December 1998 (RWQCB-USEPA 1998ab), and January 2009 (RWQCB-USEPA 2009). The October 2017 field survey described in this report was the thirty-sixth receiving-water survey conducted under the current permit.

The NPDES discharge permit requires seasonal monitoring of offshore receiving-water quality with quarterly surveys. This report summarizes the results of sampling conducted on 10 October 2017. Specifically, this fourth-quarter survey captured ambient oceanographic conditions along the central California coast during autumn. The survey's measurements were used to assess the discharge's compliance with the objectives of the California Ocean Plan (COP) and the Central Coast Basin Plan (RWQCB 1994) as promulgated by the receiving-water limitations specified in the NPDES discharge permit.

The monitoring objectives were achieved by empirically evaluating tabulations of instrumental measurements and standard field observations. In addition to the traditional, vertical water-column profiles, instrumental measurements were used to generate horizontal maps from high-resolution data gathered by towing a CTD[1] instrument package repeatedly over the diffuser structure. This allowed for a more precise delineation of the plume's lateral extent.

SURVEY SETTING

The MBCSD treatment plant is located within the City of Morro Bay, which is situated along the central coast of California halfway between Los Angeles and San Francisco. Effluent is carried from the onshore treatment plant through a 1,450-m long outfall pipe, which terminates at a diffuser structure on the seafloor 827 m from the shoreline within Estero Bay (Figure 1). The diffuser structure extends an additional 52 m toward the northwest from the outfall terminus and consists of 34 ports that are hydraulically designed to create a turbulent ejection jet that rapidly mixes effluent with receiving seawater upon discharge. Currently, six of the diffuser ports are closed, thereby improving effluent dispersion by increasing the ejection velocity from the remaining 28 ports distributed along a 42-m section of the diffuser structure.

Following discharge from the diffuser ports, additional turbulent mixing occurs as the buoyant plume of dilute effluent ascends through the water column. Most of this buoyancy-induced mixing occurs within a zone of initial dilution (ZID), whose lateral reach in modeling studies extends 15.2 m from the centerline of the diffuser structure. Beyond the ZID, energetic waves, tides, and coastal currents within Estero Bay further disperse the dilute effluent within the open-ocean receiving waters. Both vertical hydrocasts and horizontal tow surveys are conducted around the diffuser structure to assess the efficacy of the diffuser, to define the lateral extent of the discharge plume, and to evaluate compliance with the NPDES permit limitations.

[1] Conductivity, temperature, and depth (CTD)

Figure 1. Location of the Receiving-Water Survey Area

Near the diffuser, prevailing flow generally follows bathymetric contours that parallel the north-south trend of the adjacent coastline. Because of the rapid initial mixing achieved within 15 m of the diffuser structure, impingement of unmixed effluent onto the adjacent coastline, 827 m away, is highly unlikely. Nevertheless, in the event of a failure in the treatment plant's disinfection system, collection and analysis of water samples at the eight surfzone-sampling stations shown in Figure 1 would be conducted to monitor for potential shoreline impacts. These surfzone samples would be analyzed for total and fecal coliform, and enterococcus bacterial densities.

Areas of special concern, such as the Morro Bay National Estuary and the Monterey Bay National Marine Sanctuary, are not affected by the discharge because they are even more distant from the outfall location. For example, the southern boundary of the Monterey Bay National Marine Sanctuary is located 38 km to the north, while the entrance to the Morro Bay National Estuary lies 2.8 km south. The southerly orientation of the mouth of the Bay, and the presence of Morro Rock 2 km to the south, serve to further limit direct seawater exchange between the discharge point and the Bay (Figure 1).

SAMPLING LOCATIONS

As shown in Figure 2, the offshore sampling pattern consists of six fixed offshore stations located within 100 m of the outfall diffuser structure. The red ⊙ symbols in the Figure indicate the target locations of the sampling stations (Table 1). The stations are situated at three distances relative to the center of the diffuser structure, and lie along a north-south axis at the same water depth (15.2 m) as the center of the diffuser. Depending on the direction of the local oceanic currents at the time of sampling, the discharge may influence seawater properties at one or more of these stations. The up-current stations on the opposite side of the diffuser then act as reference stations. Comparisons between the water properties at these antipodal stations quantify departures from ambient seawater properties caused by the discharge and allow compliance with the NPDES discharge permit to be determined.

The finite size of the diffuser is an important consideration in the assessment of wastewater dispersion close to the discharge. Although the discharge is considered a "*point source*" for modeling and regulatory purposes, it does not occur at a single isolated point of infinitesimal size. Instead, the discharge is distributed along a 42 m section of the seafloor, and, ultimately, the amount of wastewater dispersion at a given point in the water column is dictated by its distance from the closest diffuser port, rather than its distance from the center of the diffuser structure. This "*closest approach*" distance can be considerably less than the centerpoint distance normally cited in modeling studies (compare the last two columns of Table 1).

Another important consideration for compliance evaluation is the ability to determine the actual location of the measurements. Discerning small spatial separations within the compact sampling pattern only became feasible after the advent of Differential Global Positioning Systems (DGPS). The accuracy of traditional navigation systems such as LORAN or standard GPS is typically ±15 m, a span equal to half the total width of the ZID itself. DGPS incorporates a second signal from a fixed, land-based beacon that continuously transmits position errors embedded within standard GPS readings to the DGPS receiver aboard the survey vessel. Real-time correction for these position errors provides an extremely stable and accurate offshore navigational reading with position errors of no more than 2 m, and often with sub-meter accuracy.

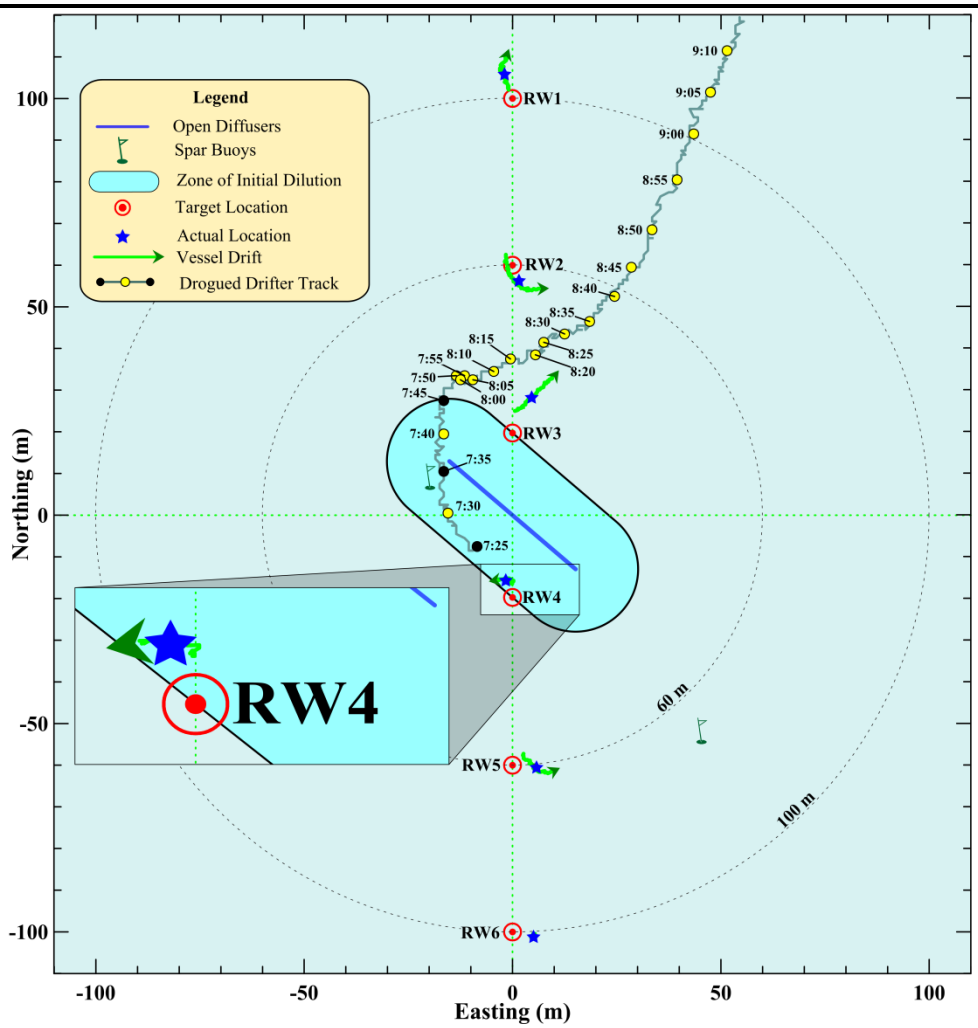

Figure 2. Station Locations

Table 1. Target Locations of the Receiving-Water Monitoring Stations

Station	Description	Latitude	Longitude	Center Distance[2] (m)	Closest Approach Distance[3] (m)
RW1	Upcoast Midfield	35° 23.253' N	120° 52.504' W	100	88.4
RW2	Upcoast Nearfield	35° 23.231' N	120° 52.504' W	60	49.4
RW3	Upcoast ZID	35° 23.210' N	120° 52.504' W	20	15.0
RW4	Downcoast ZID	35° 23.188' N	120° 52.504' W	20	15.0
RW5	Downcoast Nearfield	35° 23.167' N	120° 52.504' W	60	49.4
RW6	Downcoast Midfield	35° 23.145' N	120° 52.504' W	100	88.4

[2] Distance to the center of the open diffuser section
[3] Distance to the closest open diffuser port

During a diver survey in July 1998, the survey vessel's new DGPS navigation system, consisting of a Furuno™ GPS 30 and FBX2 differential beacon receiver, was used to precisely determine the position of the open section of the diffuser structure (MRS 1998) and establish the target locations for the receiving-water monitoring stations shown in Figure 2 and listed in Table 1. Presently, the use of two independent DGPS receivers aboard the survey vessel allows access to two separate land-based beacons for navigational intercomparison, ensuring extremely accurate and uninterrupted navigational reports.

Recording of DGPS positions at one-second intervals allows precise determination of sampling locations throughout the vertical CTD profiling conducted at the six individual stations, as well as during the tow survey. Knowledge of the precise location of individual CTD measurements relative to the diffuser is critical for accurate interpretation of the water-property fields. During vertical-profile sampling, for example, the actual measurement locations rarely coincide with the target coordinates listed in Table 1 because winds, waves, and currents induce unavoidable horizontal offsets (drift). Even during quiescent metocean[4] conditions, the residual momentum of the survey vessel as it approaches the target locations can create perceptible offsets. Using DGPS however, these offsets can be quantified, and the vessel location can be precisely tracked throughout sampling at each station.

The October 2017 hydrocasts were conducted progressing from north to south, beginning with Station RW1. The magnitude of the drift at each of the six stations during the October 2017 survey is apparent from the length of the green tracklines in Figure 2. The tracklines trace the horizontal movement of the CTD as it was lowered to the seafloor at each station. Their lengths and offsets from the target locations reflect the overall station-keeping ability during the October 2017 survey.

The time it took the CTD to traverse the water column to the seafloor, which averaged 1 min 12 s, was consistent among stations, while the lateral distance traversed by the instrument package varied considerably among the stations, ranging from less than 1 m at Station RW6, to more than 11 m at Stations RW2 and RW3 (Figure 2). Similarly, the direction of the drift was inconsistent among the stations. The lateral movement of the CTD at any given time is often determined by a complex interplay between the external influences of winds and currents, and the vessel's residual momentum immediately prior to each downcast.

However, because relatively quiescent metocean conditions prevailed during the survey, drift was primarily determined by vessel residual momentum. For example, the northward drift at Station RW1 arose from the vessel's residual momentum as it approached the station from the south. Similarly, at Stations RW2 and RW3, the respective drift directions to the south and northwest arose because of the vessel's approach from the north and southeast. In contrast, more aggressive use of reverse thrust as the vessel approached Station RW6 resulted in almost imperceptible movement of the CTD during the downcast. Metocean's secondary influence on the movement of the vessel is apparent in the curvature of the trajectories at Stations RW1, RW2, and RW5. The arc is consistent with the influence of a light onshore breeze out of the southwest[5] and a north-northeastward oceanic current flow that is reflected in the drogued-drifter trajectory in Figure 2.[6]

[4] Meteorological and oceanographic conditions include winds, waves, tides, and currents.
[5] Refer to the wind measurements in Table 4 later in this report.
[6] Refer to the partial drogued-drifter track shown in Figure 2 and the full track in Figure 3 later in this report.

Regardless of the cause, detailed knowledge of the CTD's movement during downcasts is important for the interpretation of the water-quality measurements. Because the target locations for Stations RW3 and RW4 lie along the ZID boundary (viz., the red ⊙ symbol in the inset of Figure 2), knowledge of the CTD's location during the downcasts at those stations is especially important in the compliance evaluation. This is because the receiving-water limitations specified in the COP only apply to measurements recorded along or beyond the ZID boundary, where initial mixing is assumed complete. For example, during the October 2017 survey, none of the data collected at Station RW4 was subject to a compliance assessment because the CTD remained within the ZID during the downcast, even though the CTD came within a meter of the ZID boundary as it approached the seafloor.[7] Conversely, all of the data collected at Station RW3 participated in the compliance evaluation because it was located well beyond the ZID boundary and, as it happens, directly in line with plume transport toward the northeast.

Compliance assessments notwithstanding, measurements acquired within the ZID lend valuable insight into the outfall's effectiveness at dispersing wastewater. For example, low dilution rates and concentrated effluent throughout the ZID would indicate potentially damaged or broken diffuser ports. Analysis of the outfall's operation over the past two and a half decades, however, demonstrates that it has consistently maintained a high level of effectiveness in effluent dispersal. In fact, without the occasional measurements recorded within the ZID due to vessel drift, the extremely dilute discharge plume might remain undetected within all the vertical profiles collected during a given survey.

It has not always been possible to determine which measurements were subject to permit limits among hydrocasts near the ZID boundary, however. For example, prior to 1999 and before the advent of DGPS, CTD locations could not be determined with sufficient accuracy to establish whether the average ZID station position was located within the ZID, much less, how the CTD was moving laterally during the hydrocast. Because of these navigational limitations, sampling was presumed to occur at a single, imprecisely determined, horizontal location. Federal and state reporting of monitoring data still mandates identification of a single position for all of the CTD data collected at a particular station. Thus, for regulatory reporting, and for consistency with past surveys, the October 2017 survey also identifies a single sampling location for each station. These average station positions are shown by the blue stars in Figure 2, and are listed in Table 2 along with their distances from the diffuser structure.

Table 2. Average Position of Vertical Profiles during the October 2017 Survey

	Time (PDT)				Closest Approach	
Station	**Downcast**	**Upcast**	**Latitude**	**Longitude**	**Range[8](m)**	**Bearing[9](ºT)**
RW1	8:57:30	8:58:49	35° 23.256' N	120° 52.505' W	93.9	8
RW2	9:01:42	9:02:53	35° 23.229' N	120° 52.503' W	46.5	21
RW3	9:06:00	9:07:20	35° 23.214' N	120° 52.501' W	24.6	41
RW4	9:10:39	9:11:50	35° 23.191' N	120° 52.505' W	**12.8** [10]	221
RW5	9:13:42	9:14:49	35° 23.166' N	120° 52.500' W	48.4	191
RW6	9:16:54	9:17:58	35° 23.144' N	120° 52.501' W	88.7	187

[7] The center of the green arrowhead in the inset of Figure 2 marks the location of the deepest (seafloor) measurement.
[8] Distance from the closest open diffuser port to the average profile location
[9] Angle measured clockwise relative to true north from the closest diffuser port to the average profile location
[10] All of the CTD measurements were located within the ZID boundary (refer to inset in Figure 2).

OCEANOGRAPHIC PROCESSES

The trajectory of a satellite-tracked drogued drifter measured oceanic flow throughout the October 2017 survey (Figure 3). Modeled after the curtain-shade design of Davis et al. (1982) and drogued at mid-depth (7 m), a drifter has been deployed during each of the quarterly water column surveys conducted over the past two decades. In this configuration, oceanic flow rather than surface wind dictates the drifter's trajectory, which provides a good indication of the plume's movement after discharge, except when the flow field exhibits strong vertical shear.

During the October 2017 survey, the drifter was deployed near the diffuser structure at 7:25 AM, and was recovered at 9:36 AM at a location 180 m north northeast (23°T[11]) of its original release point (red dots in Figure 3). However, the serpentine drifter route indicated that the currents that transported the drifter varied considerably during its deployment.

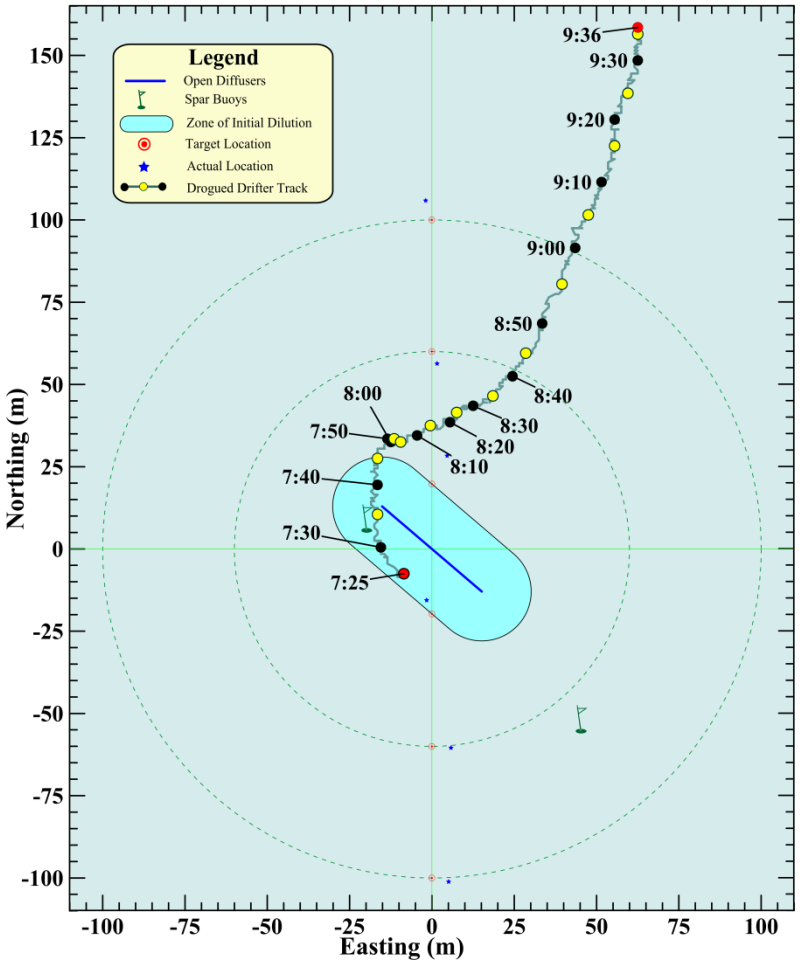

Figure 3. Drogued Drifter Trajectory

[11] Direction measured clockwise relative to true (rather than magnetic) north

For the first 24 minutes after deployment, when the first three mid-depth tow transects were conducted, the drifter travelled 40 m due north at a moderate pace of 2.8 cm/sec.[12] When the remaining mid-depth transects were conducted after 7:50 AM, the drifter remained almost motionless within a 5 m area for 17 minutes before slowly migrating toward the northeast for nearly 40 minutes. During the shallow tows and vertical casts, the oceanic flow increased in speed to 3.4 cm/sec remained consistently toward the north northeast for the remainder of the survey. The steady transport speed is reflected in the uniform spacing between the yellow and black dots in Figure 3, which show the drifter's progress at five- and ten-minute intervals.

Because of the drifter's circuitous path, it actually traversed a distance closer to 200 m as compared to the 180 m distance between the release and recovery locations. Additionally, because of changes in the speed of oceanic flow during the survey, effluent experienced varying residence times within the ZID, ranging from 7 minutes during the last part of the survey, to 52 minutes for a brief period around 8:00 AM when oceanic flow was negligible. Overall, however, the drifter trajectory accurately depicted the north northeastward transport of the effluent plume during the survey, as indicated by the northeastward offset of the plume's salinity signature that was delineated during the shallow tow survey.[13]

The correspondence between mid-depth drifter transport and shallow plume directional offset indicates that vertical shear in the flow field was minimal at the time of the October 2017 survey. Vertically uniform flow arises when barotropic oceanographic forces produce a relatively unstratified water column with vertically uniform seawater properties.[14] Tidal forcing is generally considered a barotropic process that acts on the water column as a whole. Tidal flow dominance is also consistent with the aforementioned flow stagnation around 8:00 AM that coincided with slack water that occurred after the tidal low after 7:25 AM (Figure 4). Additionally, the subsequent acceleration of drifter movement toward the north northeast (Figure 3) is consistent with the flood tide that prevailed during the rest of the survey (yellow shading in Figure 4). When other physical oceanographic influences are negligible, a flood tide tends to induce a weak northeastward (onshore) flow in the survey region, while ebb tides generate an offshore flow component.

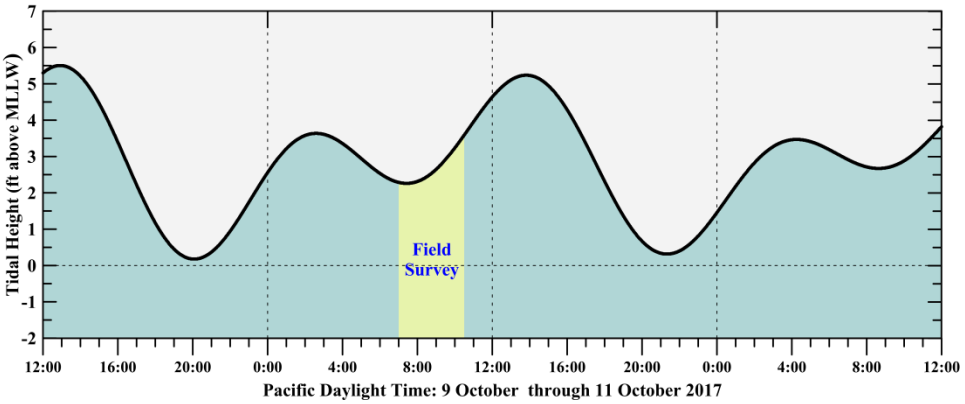

Figure 4. Tidal Level during the October 2017 Survey

Normally, however, oceanic flow near the survey area is influenced by a variety of other oceanographic processes, such as upwelling or remote processes, such as large-scale along-shore pressure gradients, or the passing of large eddies embedded within the California Current. During most surveys, vertical

[12] 0.05 kt
[13] Refer to Figure 10 later in this report.
[14] Vertical profiles at Station RW6 (see Figure 8f later in this report) were unaffected by the discharge and exhibit relatively uniform seawater properties compared to most prior surveys.

countercurrents form above and below a sharply defined thermocline in conjunction with the upwelling process. During the October 2017 survey, a slight increase in the vertical seawater-property gradients was apparent immediately above the seafloor,[15] suggesting the weak but perceptible influence of upwelling in the days prior to the survey.

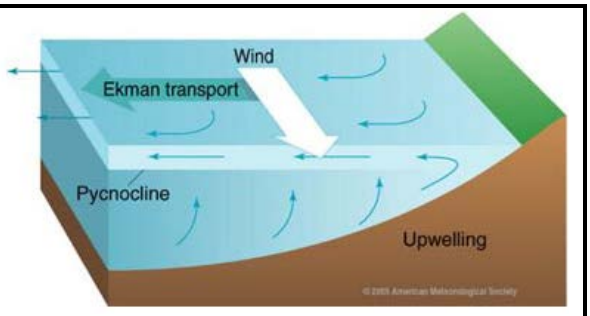

Figure 5. Schematic of Upwelling Processes

Normally, along this section of coastline, currents within the survey area are dominated by the prevailing wind field. Strong and steady northwesterly winds cause upwelling within the water column and produce a system of vertical countercurrents (Figure 5). Net flow within the upper water column, known as Ekman transport, occurs at a 90º angle to the right of the prevailing wind direction.[16] As a result, warm ocean waters within the surface mixed layer are driven offshore (southwestward) in response to the along-shore winds (toward the southeast). Near the coast, these warm surface waters are replaced by deep, cool, nutrient-rich waters that well up from below. The upwelled waters originate farther offshore and move shoreward (northeastward) along the seafloor to replace surface waters driven offshore by Ekman transport. Thus, strong upwelling establishes a vertically sheared countercurrent flow within the survey area.

The onset of these upwelling-dominated processes normally begins with a rapid intensification of southeastward-directed winds along the central coast during late March and or early April as shown by the positive (blue) upwelling indices in Figure 6. This transition to more persistent southeastward winds is initiated by the stabilization of a high-pressure field over the northeastern Pacific Ocean. Clockwise winds around this pressure field drive prevailing northwesterly winds (i.e., toward the southeast) along the central California coast. The October 2017 survey was conducted well after the onset of this spring

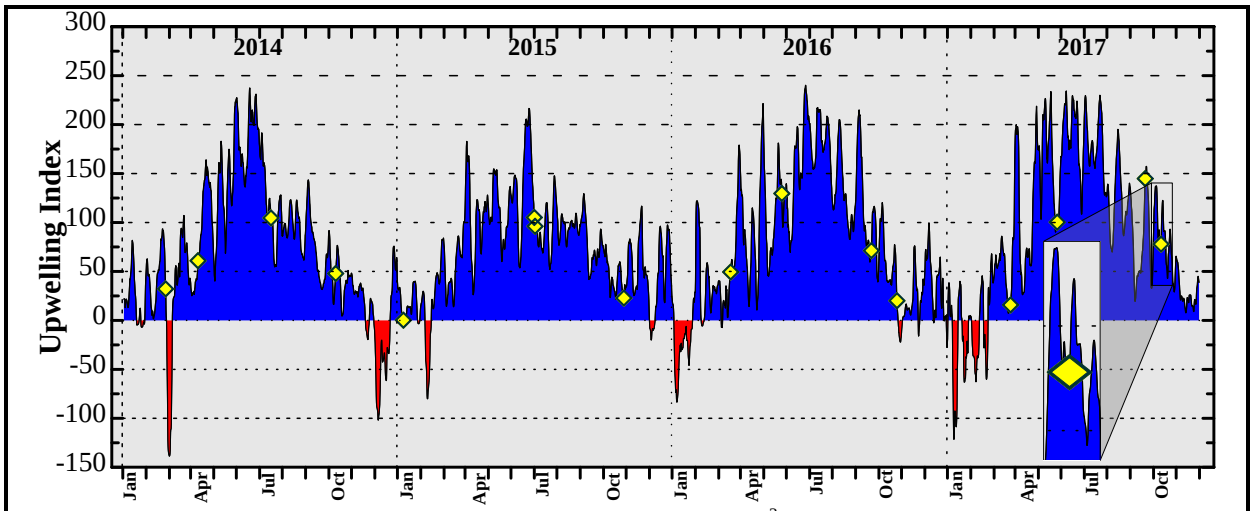

Figure 6. Five-Day Average Upwelling Index ($m^3/s/100$ m of coastline)

[15] A well-defined decline in temperature was apparent between 14.5 m and 15.5 m at the southernmost Station RW6 (red line in Figure 8f later in this report). Station RW6 was up current of the plume transport direction during the October 2017 survey and well removed from the discharge's influence. Additionally, increased vertical gradients in other seawater properties are also apparent at the same depth level suggesting a distinct watermass was present near the seafloor at the time of the survey.

[16] http://oceanmotion.org/html/background/upwelling-and-downwelling.htm

transition, and during a period when upwelling events had become weaker and less prevalent. The last yellow diamond in Figure 6 (refer to the inset) indicates that the survey was conducted when upwelling winds were weak, but were preceded by a mild wind event that peaked six days prior to the survey. The weak thermocline observed immediately above the seafloor during the October 2017 survey was probably a relic of this prior upwelling event.

Some degree of upwelling is almost always present during offshore surveys (other yellow diamonds in Figure 6). Throughout most of the year, the nutrient-rich seawater brought to the sea surface near the coast by upwelling enables phytoplanktonic blooms that are the foundation of the productive marine fishery found along the central California coast. The vertical counterflow associated with persistent upwelling conditions also enhances vertical stratification of the water column. The influx of cold dense water at depth produces a thermocline that is commonly maintained throughout summer and into early fall.

During late fall and winter, upwelling is typically weak, and occasionally downwelling events, indicated by the negative (red shaded) indices in Figure 6, occur when passing storms temporarily reverse the normal wind pattern and drive surface waters shoreward. As the surface waters approach the coastline, they downwell, producing nearly uniform seawater properties throughout the water column. An unusual series of severe winter storms at the beginning of 2017 produced multiple downwelling events (refer to the red downward excursions in the upwelling index during January and February 2017 in Figure 6).

In contrast, the weak but sustained northwesterly winds that prevailed before the October 2017 survey produced a pattern of sea surface temperatures indicative of upwelling within the central-coast oceanographic region. This upwelling pattern was captured by the satellite image shown on the cover of this report. The image was recorded by infrared sensors on one of NOAA's polar orbiting satellites during a period of relatively cloudless skies five days prior to the survey. The presence of pools of cooler, upwelled water is visually apparent immediately adjacent to the coastline (magenta shading). The 4°C difference between these sea-surface temperatures and temperatures farther offshore (in green and yellow) demonstrate that even moderate upwelling can have a profound effect on oceanographic conditions throughout the region.

METHODS

The 38 ft F/V *Bonnie Marietta*, owned and operated by Captain Mark Tognazzini of Morro Bay, served as the survey vessel on Tuesday, 10 October 2017. Douglas Coats of Marine Research Specialists (MRS) supervised scientific operations as Chief Scientist, and provided data-acquisition and navigational support during the survey. He also assisted with the deployment and recovery of the CTD and drifter, and he collected meteorological measurements at each station. Crewmember William Skok managed deck operations and collected the Secchi depth measurements at each station.

Auxiliary Measurements

Auxiliary measurements and observations were collected at each of the six stations after completion of the vertical profiling phase of the survey. Standard observations of weather and sea conditions, and beneficial uses, were augmented by visual inspection of the sea surface for floating particulates, oil sheens, and discoloration potentially related to effluent discharge. Other auxiliary measurements collected at each station included wind speeds and air temperatures measured with a handheld Holdpeak 866B Digital Thermo-Anemometer, and oceanic flow measurements made throughout the survey area using the aforementioned drogued drifter.

Additionally, at all six stations, a Secchi disk was lowered through the water column to determine its depth of disappearance. Secchi depths provide a visual measure of near-surface turbidity or water clarity.

The depth of disappearance is inversely proportional to the average amount of organic and inorganic material suspended along a line of sight in the upper water column. As such, Secchi depths measure natural light penetration, which can be limited by increased suspended particulate loads from plankton blooms, onshore runoff, seafloor sediment resuspension, and wastewater discharge. They are also biologically meaningful because the depth of the euphotic zone, where most oceanic photosynthesis occurs, is limited to approximately twice the Secchi depth.

Instrumental Measurements

A Sea Bird Electronics SBE-19plusV2 Seacat CTD instrument package collected measurements of conductivity, temperature, light transmittance, dissolved oxygen (DO), pH, and pressure during the October 2017 survey. The six seawater properties used to assess receiving-water quality in this report were derived from the continuously recorded output from the CTD's probes and sensors. Although pressure-housing limitations confine the CTD to depths less than 680 m (Table 3), this is well beyond the maximum depth of the deepest station in the outfall survey. The entire CTD was returned to the factory in January 2015 for full calibration and servicing. The transmissometer and DO probe were returned to the manufacturer in January 2016 for further servicing, repair, and calibration.

Table 3. CTD Specifications

Component	Units	Range	Accuracy	Resolution
Housing (19p-1a; Acetron Plastic)	m	0 to 680	—	—
Pump (SBE 5P)	—	—	—	—
Pressure (19p-2h; Strain-Gauge)	dBar	0 to 680	±1.7	± 0.10
Conductivity	Siemens/m	0 to 9	± 0.0005	± 0.00005
Salinity	‰	0 to 58	± 0.004	± 0.0004
Temperature	ºC	–5 to 35	± 0.005	± 0.0001
Transmissivity (WETLabs C-Star)[17]	%	0 to 100	± 0.3	± 0.03
Oxygen (SBE 43)	% Saturation	0 to 120	± 2	—
pH (SBE 18)	pH	0 to 14	± 0.1	—

The precision and accuracy of the various probes, as reported in manufacturer's specifications, are listed in Table 3. Salinity (‰) was calculated from conductivity measurements reported in units of Siemens/m. Density was derived from contemporaneous temperature (°C) and salinity data, and was expressed as 1000 times the specific gravity minus one, which is a unit of sigma-T (σ_t).

Assessments of all three of the physical parameters (salinity, temperature, and density) helped determine the lateral extent of the effluent plume during the towing phase of the survey. Additionally, during the vertical-profiling phase, they quantified layering, or vertical stratification and stability of the water column, which determines the behavior and dynamics of the effluent as it mixes with seawater within and beyond the ZID. Data on the three remaining seawater properties, light transmittance (water clarity), hydrogen-ion concentration (acidity/alkalinity – pH), and dissolved oxygen (DO), further characterized the receiving waters, and were used to assess compliance with water-quality criteria. Light transmittance was measured as a percentage of the initial intensity of a transmitted beam of light detected at the opposite end of a 0.25-m path. Transmissivity readings are reported relative to 100% transmission in air, so the maximum theoretical transmission in (pure) water is expected to be 91.3%.

Before beginning the mid-depth tow survey at 7:39 AM, the CTD was deployed beneath the sea surface for a nine-minute equilibration period as the vessel was positioned for the first transect. Prior to deployment, the CTD package had been configured for horizontal towing with forward-looking probes.

[17] 25-cm path length of red (650 nm) light

The protective cage around the CTD was fitted with a horizontal stabilizer wing and a depth-suppression weight was added to the towline to achieve near constant-depth tows.

Nine transects of mid-depth data were collected at an average depth of 8.9 m and an average speed of 1.68 m/s over the span of 33 minutes (blue-green lines in Figure 7). Subsequently, at 8:14 AM, nine additional passes were made with the CTD at an average depth of 2.9 m (orange lines). During this 28-minute shallow tow, vessel speed averaged 1.74 m/s.

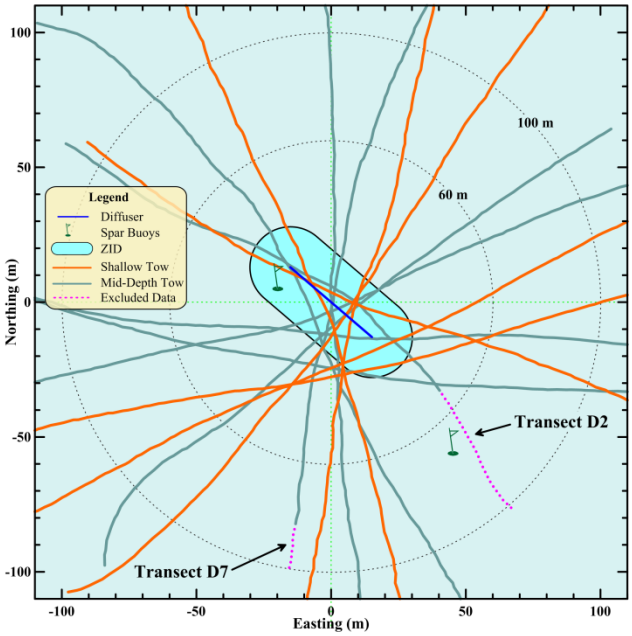

Figure 7. CTD Tracklines during the October 2017 Tow Surveys

At the observed towing speeds and the 4 Hz sampling rate, at least 2.3 CTD measurements were collected for each meter traversed. This complies with the NPDES discharge permit requirement for minimum horizontal resolution of at least one sample per meter during at least five passes around and across the ZID at two separate depths, one within the surface mixed layer and one at mid-depth within the thermocline. Contemporaneous navigation fixes recorded aboard the survey vessel were adjusted for CTD setback and aligned with time stamps on the internally recorded CTD data. The resulting data for the six seawater properties were then processed to produce horizontal maps within the upper and sub-thermocline portions of the water column.[18]

At 8:42 AM, following completion of the last shallow transect, the CTD package was brought aboard the survey vessel and reconfigured for vertical profiling. The CTD was redeployed at 8:52 AM, and was held beneath the surface for three minutes as the vessel was repositioned over Station RW6. The CTD was then raised to within 0.5 m of the sea surface and profiling commenced. The CTD was lowered at a continuous rate of speed to the seafloor. Measurements at all six stations were collected during a single deployment of the CTD package by towing it below the ocean surface while transiting between adjacent stations.

Quality Control

During the vertical-profiling and horizontal-towing phases of the survey, real-time data were monitored for completeness and range acceptability. Although real-time monitoring indicated that the recorded properties were complete and within acceptable coastal seawater ranges,[19] subsequent post-processing revealed events that impacted portions of the data, resulting in the adjustment or exclusion of these data prior to initiating the compliance analysis. As in prior surveys, review of the tow data revealed that the CTD changed depth when the vessel executed a turn at the end of each transect. These vertical offsets in CTD depth are introduced by changes in vessel speed and direction that are instituted to realign the vessel between each transect. Because of the complex interaction between turn radius, vessel speed, and CTD depth, the CTD's target depth cannot always be maintained at these times.

[18] Figures 9 and 10 later in this report

[19] Field sampling protocols employed during the survey generally followed the field operations manual for the Southern California Bight Study (SCBFMC 2002), which includes CTD cast-acceptability ranges listed in Table 2 of the manual.

Because the discharge-related anomalies used in the compliance analysis are identified by comparing the amplitudes of measurements acquired at the same depth level, the ability to resolve anomalies with statistical certainty is compromised when data from different depth levels are combined in the horizontal maps. This is particularly true when the water column is strongly stratified, but remains a concern even in the presence of weak stratification, as was the case during the October 2017 survey. However, only small portions of two transects (D2 and D7) exhibited unacceptable depth offset due to turning within the 100-m survey area (purple dotted lines in Figure 7).

Additionally, the pH sensor experienced an unusually extended equilibration period that affected the accuracy of the raw CTD data collected during the first mid-depth tow transect (D1), and to a lesser extent the initial portion of second transect (D2). The pre-survey soak period was too brief to provide full equilibration, and pH readings were artificially elevated during these two transects. Fortunately, the equilibration process produced a steady temporal decline in pH offset that could be accurately characterized by fitting an orthogonal polynomial to the pH time series from this initial portion of the mid-depth tow data.

Temporal correction of pH data and exclusion of small portions of data due to depth offset did not adversely affect the compliance analysis, however. The pH correction was small within the 100-m survey area, and the largest reduction of less than 0.085 pH units only occurred along the initial portion of Transect D1. Similarly, the small portions of excluded depth-offset data were located south of the discharge, and in an area up current of plume transport.[20] Moreover, the remaining transects were long enough to fully encompass the 100-m survey area surrounding the diffuser structure. Specifically, the tow data that was included in the compliance analysis, shown by the solid orange and blue-green lines in Figure 7, met the permit monitoring requirement of at least five passes near the diffuser structure at each tow depth.

RESULTS

The fourth-quarter receiving-water survey was conducted on the morning of Tuesday, 10 October 2017. The receiving-water survey commenced at 7:25 AM with the deployment of the drogued drifter. Over the ensuing two hours and eleven minutes, offshore observations and measurements were collected as required by the NPDES monitoring program. The survey ended at 9:36 AM with the retrieval of the drogued drifter. Collection of required visual observations of the sea surface was unencumbered throughout the survey.

Auxiliary Observations

On the morning of 10 October 2017, skies were clear, with a sustained gentle alongshore breeze out of the southwest (Table 4). Auxiliary observations were collected beginning at 9:25 AM, after completion of the vertical profiling phase of the survey. During the subsequent eleven minutes, each station was re-occupied beginning with Station RW6. After auxiliary observations were collected at Station RW6, stations were sampled sequentially progressing toward the north. During that time, wind speed and air temperature remained relatively constant. A swell out of the northwest had a significant wave height of one-to-two feet. At 21°C, average air temperature was significantly warmer than the 13.7°C sea surface temperature.

There was no evidence of floating particulates, oil sheens, or any discoloration of the sea surface associated with the presence of wastewater constituents. There was no other visual indication of the presence of the discharge plume at or beneath the sea surface during the survey. Ambient light penetration beneath the sea surface was limited by a dense population of planktonic organisms within the upper half of the water column. During upwelling in the week prior to the survey, nutrients carried upward into the

[20] Compare the southern location of the dotted lines in Figure 7 with the largely northward drifter transport in Figure 3.

Table 4. Standard Meteorological and Oceanographic Observations

Station	Location[21]		Diffuser Distance	Time	Air	Cloud Cover	Wind Avg	Wind Dir (from)	Swell Ht/Dir	Secchi Depth
	Latitude	Longitude	(m)	(PDT)	(°C)	(%)	(kt)	(°T)	(ft/°T)	(m)
RW1	35° 23.256' N	120° 52.499' W	94.4	9:36:18	20.8	0%	3.3	220	1-2 NW	4.0
RW2	35° 23.235' N	120° 52.505' W	55.7	9:34:50	20.3	0%	3.8	220	1-2 NW	3.8
RW3	35° 23.214' N	120° 52.502' W	23.4	9:31:55	19.7	0%	3.4	215	1-2 NW	3.8
RW4	35° 23.190' N	120° 52.504' W	12.3	9:29:46	20.0	0%	3.1	210	1-2 NW	3.8
RW5	35° 23.175' N	120° 52.503' W	34.4	9:27:55	19.1	0%	3.3	220	1-2 NW	3.0
RW6	35° 23.148' N	120° 52.502' W	82.7	9:25:46	18.5	0%	3.6	220	1-2 NW	3.0

euphotic zone are assimilated by phytoplankton, whose populations increase and, along with their associated zooplanktonic herbivores; their elevated densities reduce the transmittance of ambient light.

Because of the plankton-induced turbidity increase, the Secchi disk faded from view at a relatively shallow depth of 3 m as it was lowered through the upper water column at stations largely unaffected by the plume (Stations RW5 and RW6 in Table 4). The measured Secchi depth indicates that a 6-m euphotic zone was present during the survey, and that ambient light only penetrated through the upper third of the water column and did not extend to the 8.9-m level where the mid-depth tow was conducted. However, as will be discussed subsequently, the plume carried clearer ambient seawater to the sea surface as it rose through the water column at Stations RW1 through RW4. The associated increased water clarity within the upper water column resulted in a 0.8-to-1 m increase in Secchi depth measured at those stations (Table 4). Increased Secchi depth and instrumental measurements that indicated the plume reached the sea surface notwithstanding, there was no obvious visual expression of the plume at the sea surface. Similarly, no evidence of floating particulates, oil sheens, or any discoloration of the sea surface was visually apparent during the survey that might be potentially related to the presence of wastewater constituents.

Communication with plant personnel and subsequent review of effluent discharge properties around the time of the survey, confirmed that the treatment process was performing well. The 0.802 million gallons of effluent discharged on 10 October had a temperature of 22°C, a pH of 7.3, and a suspended-solids concentration of 31 mg/L. An effluent sample collected on 11 October, the day after the survey, had a biochemical oxygen demand (BOD) of 38 mg/L. The oil and grease concentration measured within effluent discharged on the day of survey was estimated to be 1.2 mg/L, but was too low to be reliably quantified.

Instrumental Observations

Data collected during vertical profiling were processed in accordance with standard procedures (SCCWRP 2002), and are collated at 0.5-m depth intervals in Table 5. Data collected during the October 2017 survey reflect weakly stratified conditions within Estero Bay indicative of a relaxation in coastal upwelling following a brief pulse of upwelling wind of limited strength (refer to the inset in Figure 6). As described previously, upwelling of varying intensity occurs most of the year along the central California coast, with the strongest upwelling winds beginning in March or April and extending through the summer. The intensity of upwelling tends to decline into fall, although pulses of sustained northwesterly winds still occur. An intense upwelling event results in the rapid influx of dense, cold, saline water at depth and leads to a sharp thermocline, halocline, and pycnocline where temperature, salinity, and density change rapidly over a small vertical distance. Under these highly stratified conditions, isotherms crowd together to form

[21] Locations are the vessel positions at the time the Secchi depths were measured. These depart from the CTD profile locations listed in Table 2 because they were collected after completion of the CTD profiling.

Table 5. Vertical Profile Data Collected on 10 October 2017

Depth (m)	Temperature (°C)						Salinity (‰)					
	RW-1	RW-2	RW-3	RW-4	RW-5	RW-6	RW-1	RW-2	RW-3	RW-4	RW-5	RW-6
0.5	13.663	13.670	13.565	13.645	13.712	13.855	33.403	33.405	33.381	33.369	33.410	33.453
1.0	13.659	13.659	13.584	13.723	13.711	13.860	33.407	33.404	33.375	33.426	33.408	33.455
1.5	13.648	13.648	13.604	13.732	13.730	13.845	33.410	33.401	33.377	33.439	33.418	33.454
2.0	13.641	13.645	13.604	13.744	13.751	13.806	33.412	33.400	33.381	33.452	33.429	33.451
2.5	13.627	13.655	13.576	13.746	13.757	13.785	33.412	33.407	33.374	33.453	33.432	33.452
3.0	13.641	13.682	13.583	13.747	13.772	13.775	33.419	33.422	33.380	33.453	33.450	33.452
3.5	13.644	13.706	13.582	13.751	13.764	13.760	33.420	33.434	33.387	33.453	33.453	33.452
4.0	13.659	13.708	13.586	13.751	13.754	13.748	33.425	33.435	33.397	33.453	33.453	33.452
4.5	13.679	13.708	13.588	13.751	13.748	13.738	33.431	33.435	33.405	33.453	33.453	33.452
5.0	13.692	13.705	13.636	13.750	13.738	13.734	33.435	33.433	33.432	33.453	33.453	33.453
5.5	13.691	13.707	13.658	13.748	13.736	13.735	33.434	33.436	33.445	33.452	33.453	33.453
6.0	13.692	13.710	13.661	13.741	13.739	13.730	33.434	33.442	33.447	33.452	33.454	33.453
6.5	13.697	13.710	13.665	13.727	13.739	13.726	33.436	33.448	33.446	33.452	33.453	33.453
7.0	13.720	13.707	13.667	13.725	13.738	13.726	33.445	33.450	33.446	33.453	33.453	33.454
7.5	13.736	13.702	13.664	13.725	13.736	13.724	33.450	33.450	33.447	33.453	33.453	33.453
8.0	13.734	13.695	13.671	13.724	13.738	13.714	33.449	33.450	33.449	33.454	33.454	33.452
8.5	13.728	13.693	13.671	13.725	13.737	13.706	33.449	33.450	33.448	33.454	33.454	33.451
9.0	13.696	13.692	13.668	13.723	13.730	13.703	33.442	33.450	33.449	33.454	33.453	33.450
9.5	13.672	13.692	13.667	13.724	13.725	13.705	33.436	33.450	33.449	33.454	33.454	33.451
10.0	13.669	13.685	13.666	13.719	13.720	13.697	33.437	33.450	33.449	33.454	33.453	33.450
10.5	13.668	13.677	13.669	13.683	13.716	13.689	33.438	33.450	33.449	33.451	33.454	33.449
11.0	13.678	13.631	13.670	13.657	13.712	13.691	33.444	33.446	33.449	33.450	33.454	33.450
11.5	13.683	13.600	13.665	13.622	13.694	13.685	33.445	33.445	33.450	33.448	33.453	33.451
12.0	13.684	13.592	13.645	13.551	13.628	13.651	33.447	33.446	33.449	33.443	33.447	33.448
12.5	13.662	13.589	13.615	13.544	13.565	13.634	33.447	33.447	33.448	33.445	33.444	33.449
13.0	13.622	13.585	13.582	13.543	13.526	13.616	33.445	33.447	33.446	33.446	33.444	33.447
13.5	13.611	13.574	13.577	13.542	13.506	13.607	33.446	33.446	33.446	33.446	33.445	33.447
14.0	13.595	13.553	13.567	13.540	13.475	13.600	33.445	33.446	33.446	33.446	33.445	33.448
14.5	13.577	13.528	13.522	13.526	13.440	13.552	33.445	33.446	33.445	33.446	33.446	33.446
15.0	13.530	13.483	13.457	13.475	13.398	13.445	33.445	33.445	33.445	33.446	33.446	33.444
15.5	13.458	13.449	13.392	13.415	13.339	13.320	33.446	33.446	33.445	33.445	33.445	33.443
16.0		13.503	13.370	13.354	13.294	13.301		33.451	33.447	33.446	33.447	33.446
16.5				13.355						33.460		

Table 5. Vertical Profile Data Collected on 10 October 2017 (continued)

Depth (m)	Density (σ_t)						pH					
	RW-1	RW-2	RW-3	RW-4	RW-5	RW-6	RW-1	RW-2	RW-3	RW-4	RW-5	RW-6
0.5	25.023	25.022	25.026	24.963	25.018	25.022	8.087	8.083	8.072	8.080	8.099	8.126
1.0	25.026	25.024	25.017	25.028	25.017	25.022	8.089	8.087	8.072	8.092	8.099	8.127
1.5	25.031	25.024	25.015	25.036	25.020	25.024	8.088	8.086	8.073	8.100	8.099	8.128
2.0	25.034	25.024	25.017	25.044	25.025	25.031	8.089	8.085	8.075	8.107	8.106	8.127
2.5	25.037	25.027	25.018	25.045	25.025	25.035	8.089	8.086	8.075	8.108	8.109	8.127
3.0	25.039	25.033	25.021	25.044	25.036	25.037	8.089	8.092	8.073	8.110	8.114	8.126
3.5	25.039	25.038	25.027	25.044	25.040	25.040	8.091	8.096	8.073	8.110	8.117	8.123
4.0	25.040	25.038	25.034	25.043	25.043	25.043	8.091	8.098	8.075	8.110	8.118	8.118
4.5	25.041	25.038	25.039	25.043	25.044	25.045	8.093	8.099	8.074	8.110	8.115	8.115
5.0	25.042	25.037	25.050	25.043	25.046	25.047	8.095	8.099	8.076	8.111	8.114	8.114
5.5	25.041	25.039	25.056	25.043	25.047	25.047	8.095	8.098	8.082	8.110	8.112	8.112
6.0	25.041	25.043	25.057	25.045	25.046	25.048	8.098	8.097	8.088	8.109	8.111	8.110
6.5	25.041	25.048	25.055	25.048	25.046	25.049	8.096	8.100	8.091	8.108	8.112	8.110
7.0	25.043	25.050	25.055	25.049	25.046	25.049	8.096	8.098	8.090	8.107	8.111	8.110
7.5	25.044	25.051	25.056	25.049	25.047	25.049	8.099	8.099	8.091	8.107	8.111	8.110
8.0	25.044	25.052	25.056	25.049	25.046	25.050	8.101	8.098	8.091	8.107	8.112	8.107
8.5	25.045	25.053	25.056	25.049	25.046	25.051	8.102	8.097	8.091	8.108	8.111	8.104
9.0	25.046	25.053	25.057	25.049	25.048	25.051	8.100	8.096	8.093	8.105	8.110	8.100
9.5	25.046	25.053	25.058	25.049	25.049	25.051	8.098	8.095	8.092	8.105	8.110	8.100
10.0	25.048	25.054	25.058	25.050	25.050	25.052	8.094	8.095	8.092	8.106	8.107	8.098
10.5	25.049	25.056	25.057	25.056	25.051	25.052	8.092	8.095	8.092	8.105	8.106	8.095
11.0	25.051	25.062	25.057	25.060	25.052	25.053	8.092	8.091	8.092	8.099	8.103	8.093
11.5	25.051	25.068	25.058	25.066	25.055	25.056	8.092	8.087	8.091	8.093	8.104	8.092
12.0	25.052	25.071	25.062	25.076	25.064	25.060	8.093	8.085	8.092	8.086	8.100	8.092
12.5	25.057	25.071	25.067	25.079	25.074	25.064	8.094	8.081	8.091	8.081	8.092	8.092
13.0	25.063	25.072	25.072	25.080	25.082	25.066	8.091	8.082	8.087	8.080	8.083	8.087
13.5	25.066	25.074	25.074	25.080	25.087	25.068	8.087	8.082	8.081	8.079	8.077	8.084
14.0	25.069	25.078	25.076	25.081	25.094	25.070	8.085	8.080	8.081	8.080	8.074	8.085
14.5	25.073	25.083	25.084	25.084	25.101	25.079	8.086	8.079	8.080	8.079	8.071	8.082
15.0	25.082	25.092	25.097	25.094	25.110	25.098	8.082	8.075	8.076	8.077	8.067	8.080
15.5	25.097	25.100	25.110	25.106	25.121	25.123	8.067	8.064	8.063	8.068	8.058	8.073
16.0		25.100	25.116	25.119	25.131	25.129		8.065	8.055	8.053	8.050	8.048
16.5				25.119						8.051		

Table 5. Vertical Profile Data Collected on 10 October 2017 (continued)

Depth (m)	Dissolved Oxygen (mg/L)						Transmissivity (%)					
	RW-1	RW-2	RW-3	RW-4	RW-5	RW-6	RW-1	RW-2	RW-3	RW-4	RW-5	RW-6
0.5	8.231	8.259	8.021	8.321	8.289	8.747	80.219	80.156	80.937	78.146	77.856	77.411
1.0	8.229	8.163	8.078	8.473	8.528	8.768	80.436	80.403	80.687	76.327	78.018	78.274
1.5	8.225	8.180	8.053	8.495	8.556	8.754	80.019	80.640	80.698	75.829	78.013	78.237
2.0	8.197	8.242	8.000	8.484	8.618	8.717	79.939	80.793	80.659	75.631	77.267	77.674
2.5	8.248	8.345	8.026	8.494	8.635	8.646	79.871	80.854	80.497	75.235	76.852	75.384
3.0	8.240	8.370	8.021	8.513	8.590	8.571	79.892	80.327	80.972	75.343	75.927	73.182
3.5	8.298	8.362	8.041	8.495	8.566	8.530	79.805	79.520	80.746	75.634	74.293	73.371
4.0	8.322	8.349	8.070	8.508	8.518	8.511	79.680	78.243	80.582	75.730	74.324	73.676
4.5	8.330	8.354	8.202	8.505	8.488	8.499	79.325	77.653	80.794	75.296	74.487	74.173
5.0	8.318	8.361	8.234	8.494	8.507	8.495	78.918	77.808	80.865	75.123	74.608	74.241
5.5	8.326	8.362	8.231	8.453	8.511	8.479	78.820	77.824	81.157	75.331	75.252	74.228
6.0	8.364	8.339	8.244	8.424	8.513	8.489	78.566	77.868	81.586	75.306	75.382	74.380
6.5	8.409	8.324	8.247	8.443	8.494	8.468	78.739	78.026	81.586	75.597	75.159	74.788
7.0	8.391	8.296	8.233	8.449	8.492	8.411	78.774	78.385	81.261	75.312	75.001	74.968
7.5	8.389	8.301	8.238	8.437	8.511	8.312	78.182	79.055	81.204	75.388	74.993	74.819
8.0	8.301	8.298	8.245	8.432	8.483	8.288	77.821	79.600	81.348	75.071	75.096	75.798
8.5	8.221	8.302	8.244	8.430	8.437	8.288	77.805	80.139	81.166	75.179	75.375	76.420
9.0	8.223	8.301	8.236	8.432	8.399	8.278	78.492	80.529	81.178	75.241	75.218	78.252
9.5	8.215	8.271	8.232	8.374	8.382	8.251	80.245	80.657	81.221	75.413	75.417	79.810
10.0	8.225	8.221	8.248	8.256	8.363	8.247	81.255	80.676	81.273	75.604	75.808	79.377
10.5	8.233	8.108	8.248	8.220	8.338	8.236	81.253	81.128	81.236	75.800	76.637	79.983
11.0	8.254	8.099	8.202	8.128	8.191	8.182	81.375	81.839	81.339	78.669	76.910	81.334
11.5	8.217	8.095	8.167	8.054	8.041	8.138	81.863	82.884	81.615	81.040	77.006	80.754
12.0	8.145	8.089	8.112	8.059	7.998	8.120	81.602	83.340	81.643	84.361	78.472	80.189
12.5	8.142	8.085	8.071	8.060	7.975	8.097	81.671	83.970	82.624	85.867	82.808	81.842
13.0	8.146	8.069	8.071	8.051	7.915	8.100	83.169	83.890	83.881	86.245	85.969	82.744
13.5	8.134	8.003	8.071	8.052	7.835	8.060	84.954	84.303	84.592	86.398	86.681	82.844
14.0	8.065	7.925	7.928	7.977	7.719	7.789	85.250	85.194	84.854	86.328	86.398	83.501
14.5	7.845	7.734	7.678	7.832	7.605	7.542	85.230	85.569	85.237	86.570	86.080	83.403
15.0	7.701	7.709	7.617	7.700	7.475	7.403	85.437	85.380	84.695	86.663	85.513	84.542
15.5	7.784	7.912	7.623	7.514	7.426	7.432	84.574	84.814	81.385	86.119	84.421	85.581
16.0		7.747	7.623	7.639	7.492	7.699		85.235	81.551	85.395	83.653	83.200
16.5				7.539						85.395		

a density interface that inhibits the vertical exchange of nutrients and other water properties, traps the effluent plume at depth, and reduces the initial dilution of the effluent plume.

If the upwelling winds are only of moderate strength, occur only briefly, or have not occurred recently; then vertical mixing slowly erodes the sharp contrast between the surface and deep watermasses. As a result, stratification appears as a more gradual vertical change in seawater properties that can eventually extend throughout the entire water column. At the time of the October 2017 survey, vertical mixing had largely eroded the moderate stratification generated by a recent prior upwelling event. The resulting weak vertical gradients are apparent in the profiles measured at the southernmost Station RW6 (Figure 8f). Station RW6 was located up current from the discharge point, and therefore, it was well removed from the influence of effluent discharge. Thus, the profiles at that station reflect the ambient stratification present at the time of the survey. The profiles reveal that most seawater properties steadily changed with depth throughout the upper 13.5 m of the water column, and exhibited slightly increased gradients immediately above the seafloor. The diffuse transition that was present throughout most of the water column was probably composed of eroded remnants from a more sharply defined mid-depth thermocline generated by the upwelling event in the days prior to the survey.

Regardless of the upwelling-event intensity, or the lapse in time since the event, regional upwelling events produce predicable vertical trends in seawater properties within the survey area. Namely, most seawater properties exhibit steadily increasing or decreasing values with depth that are determined by well-established physicochemical processes within ocean waters. These processes are evident in the seawater-property trends shown in Figure 8f even though intense upwelling winds had largely dissipated by the time of the survey. Specifically, temperature (red line), DO (dark blue line), and pH (olive-colored line) steadily decrease with depth down to 13.5 m. These decreases are mirrored by a density profile (black line) that steadily increases with depth.

Thus, the water-property distribution throughout most of the water column constitutes a gradual transition zone from warm well-oxygenated sea-surface conditions to dissimilar conditions associated with a distinct watermass that was present near the seafloor. The seafloor watermass migrated shoreward along the seafloor as part of the upwelling process and carried cold, nutrient-rich but oxygen-poor seawater that reflect conditions typical of its origin deep offshore. Within the survey area, the remnants of this deep offshore watermass become most apparent below 13.5 m. This 2.5-m thick bottom layer contained seawater that was colder and denser than shallow waters. As a result, temperatures decrease (red line) and density increases (black line) with increasing depth within the overlying transition zone (Figure 8f). Similarly, the deep watermass had not been in recent direct contact with the atmosphere, and biotic respiration and decomposition had depleted its DO levels (dark blue line). Biotic respiration and decomposition also produces carbon dioxide (CO_2), and in its dissolved state, the increased concentration of carbonic acid appears as a concomitant reduction in pH (olive-colored line).

Although these vertical trends in seawater properties within the transition zone were well defined, the magnitudes of the vertical gradients were small compared to those of most other surveys. These gradual trends reflect a water column that was only weakly stratified at the time of the October 2017 survey. This weak stratification profoundly affected the dynamics of effluent dispersion. During most other surveys, when the water column is strongly stratified by recent upwelling, the rising plume becomes trapped at depth within the water column, thereby limiting its full capacity for dilution. In contrast, during the October 2017 survey, the plume rose all the way to the sea surface. The surface signature of the effluent plume was unmistakably confirmed by marked salinity reductions at all five of the other stations (shown by green shading Figure 8abcde). Additionally, at those stations, the gradual vertical gradients seen in other water properties within the upper half of the ambient water column at Station RW6 (Figure 8f), were largely eliminated by the rising effluent plume. Specifically, seafloor entrainment and upward transport of

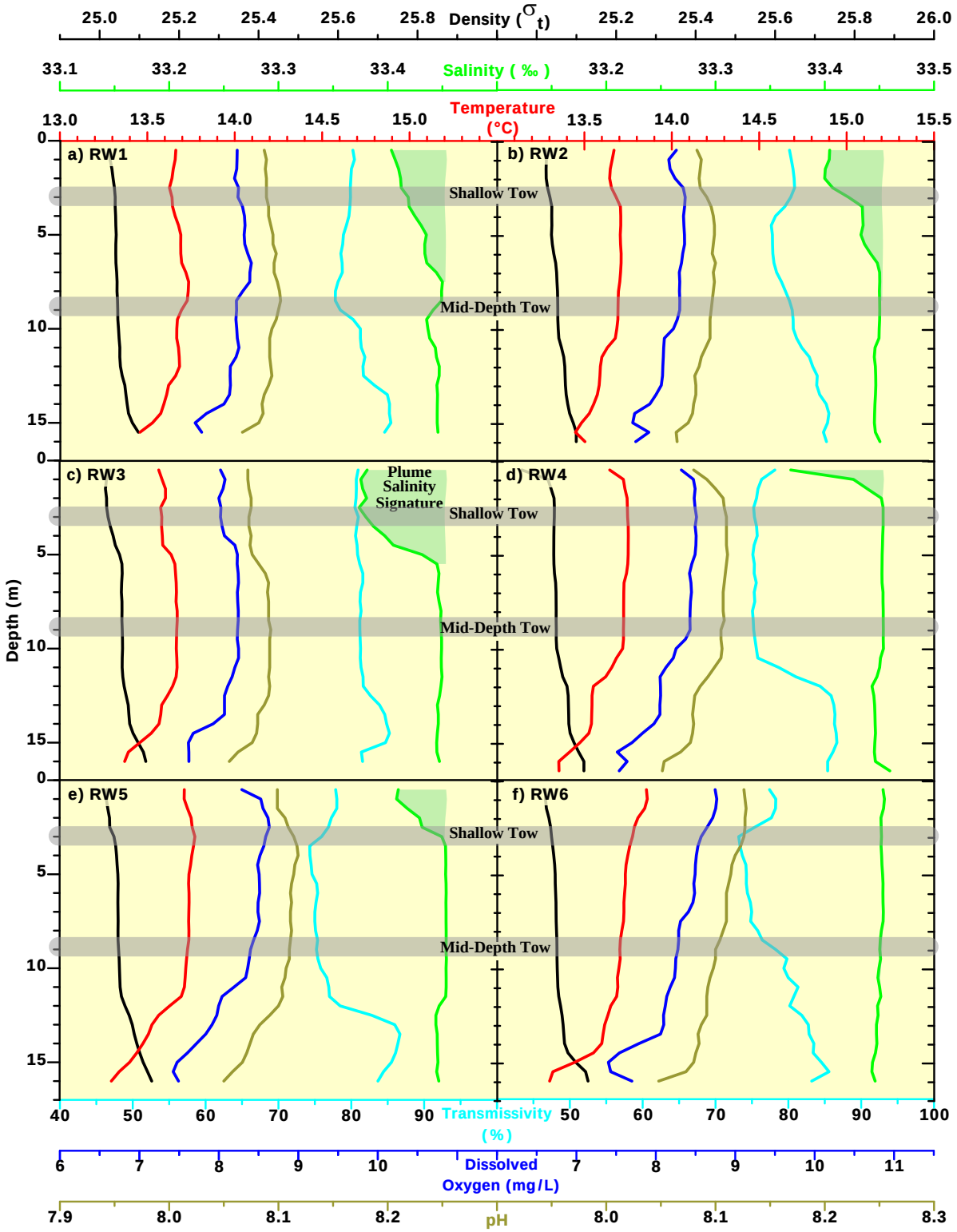

Figure 8. Vertical Profiles of Water-Quality Parameters

deep ambient seawater within the rising plume produced nearly uniform seawater properties throughout the upper water column.

Because of the water column's weak stratification at the time of the October 2017 survey, the plume rose rapidly through the water column and impinged on the sea surface, whereupon it spread laterally. Additionally, because prevailing oceanic currents were weak, they provided little additional spreading and mixing during the plume's rapid rise. As a result, the rising plume's low salinity signature was largely restricted to a highly localized area directly over the diffuser structure, and only began to become apparent immediately beneath the sea surface as it spread laterally and reached the locations of the stations. This is apparent in the green shading in Figure 8abcde, which was largely restricted to depths above approximately 5 m. As shown by the lower, thick shaded horizontal line superimposed on the vertical profiles in Figure 8, the 8.9 m mid-depth tow was located beneath this plume-spreading zone.

Accordingly, the mid-depth salinity map (Figure 9b) delineated the rising plume's signature only within a very limited area centered on the diffuser structure. Localized anomalies in temperature, density, DO, and pH (Figure 9acef) coincided spatially with the salinity anomaly, further confirming the location and extent of the rising plume. However, in contrast to the plume's reduced salinity, which reflects the presence of dilute wastewater constituents, these other water-property anomalies were generated by entrainment of ambient seawater near the seafloor. As described previously with regard to vertical profile data in Figure 8, the plume entrained deep ambient seawater shortly after discharge. This deep ambient seawater was colder, less oxygenated, and more acidic immediately above the seafloor as compared to the overlying seawater (Figure 8f). Upward transport of this entrained seawater within the rising effluent plume resulted in vertical profiles that were nearly uniform (Figure 8abcde). When viewed on a horizontal map, the anomalies appear as localized reductions in temperature, DO, and pH (Figure 9aef).

The mid-depth spatial distribution of the two remaining properties, density and transmissivity, lend additional insight into plume dynamics. A well-delineated density reduction associated with the rising plume immediately above the diffuser structure coincided spatially with anomalies in the properties described above (compare Figure 9c with Figure 9abef). However, in contrast to the thermal, DO, and pH anomalies, the density anomaly was not generated by entrainment. Instead, because the density within the plume was lower than the surrounding seawater at mid-depth, it could only have resulted from the presence of dilute effluent. In fact, density is not an independent seawater parameter and is instead determined by the seawater equation of state that relates density to salinity, among other parameters. Thus, the reduced salinity associated with the plume's dilute wastewater constituents in Figure 9b, also resulted in the reduced density in Figure 9c. Additionally, the plume had lower density than the surrounding waters, which indicates that the plume was buoyant at mid-depth, and that it would continue to rise within the water column. This is an important consideration for compliance analysis because receiving-water limitations are imposed at the completion of the initial dilution process, which includes the additional turbulent mixing generated by the plume's rise through the water column.

The transmissivity distribution at mid-depth was diffuse and did not exhibit an anomaly that coincided with the plume signature seen in other water properties (Figure 9d). In contrast to the other properties, the vertical transmissivity gradient below 9 m was small (light blue line in Figure 8f). The increased transmissivity (water clarity) within the seawater entrained at depth appears to have counteracted the slightly reduced water clarity resulting from the presence of wastewater particulates within the plume at mid depth. However, as the plume continued to rise through the water column, it further diluted wastewater particulates and entrained seawater with relatively high water clarity.

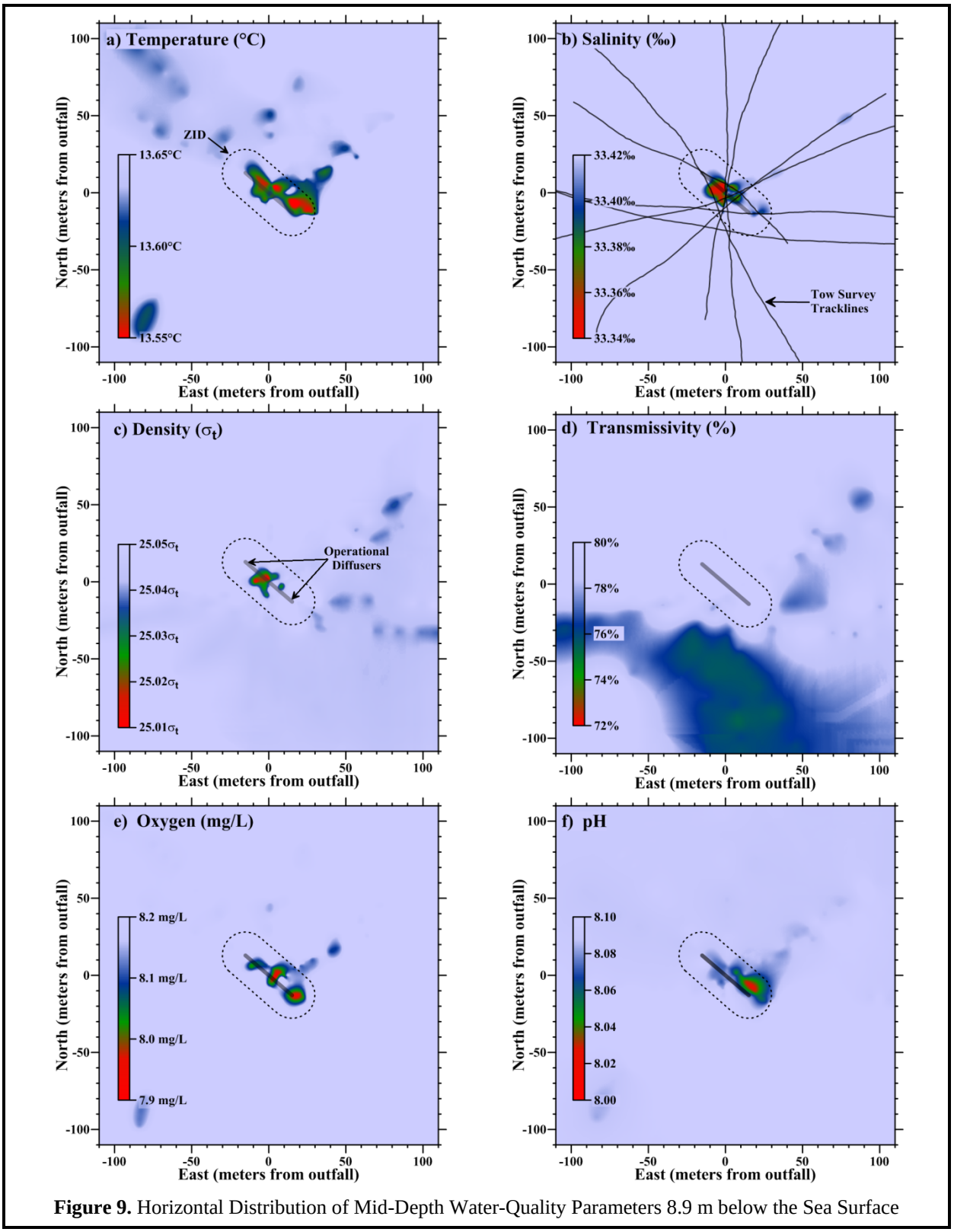

Figure 9. Horizontal Distribution of Mid-Depth Water-Quality Parameters 8.9 m below the Sea Surface

As the plume approached the sea surface and entered the euphotic zone, it encountered ambient seawater that was naturally more turbid due to the increased plankton concentration (lower transmissivity near the 3-m shallow-tow depth shown by the light-blue line in Figure 8f). The resulting contrast between plume and ambient transmissivity formed a strong transmissivity anomaly that clearly delineated the lateral extent of the plume in the shallow-tow map (Figure 10d). Because the plume had higher water clarity than surrounding seawater at this depth, the plume's transmissivity anomaly could not have been generated by turbidly associated with dilute wastewater particulates (note the reversed scale in Figure 10d).

In fact, all the seawater properties exhibit plume-related anomalies that clearly delineate its lateral transport and spreading near the sea surface (Figure 10). All exhibit extrema directly over the diffuser structure with spreading toward the north northeast; in a direction consistent with transport by prevailing currents that were measured by the drogued drifter (Figure 3). As with transmissivity, the lower temperatures measured within the plume (Figure 10a) could not have been generated by the presence of warmer wastewater. Instead, the shallow anomalies observed in all the seawater properties except salinity and density arose from the entrainment of deep ambient seawater within the rising plume.

Because entrainment anomalies are generated by the physical movement of ambient seawater, and not plume-dilution processes, they can be particularly long lived, and can remain apparent long after the wastewater constituents have dispersed far beyond recognition. This is reflected in the difference between the plume-signature patterns associated with the salinity and density distributions (Figure 10bc), as compared to those of the other seawater properties (Figure 10 adef). The entrainment-generated anomalies remain readily apparent over a wide area that extends more than 100 m north northeast of the discharge, while the salinity anomaly, which reflects actual wastewater concentration, is barely perceptible beyond the ZID.

In addition to their longevity, entrainment generated anomalies are only apparent when the water column is sufficiently stratified to cause a perceptible contrast between the shallow and deep ambient seawater properties within the rising plume. Only then does the initial dilution process produce entrainment anomalies. Initial dilution begins with intense mixing that is driven by the momentum of the effluent's ejection from the individual diffuser ports. Subsequent turbulent mixing caused by the plume's ascent through the water column is less intense, and as a result, the dilute effluent plume tends to retain the ambient seawater properties it acquired near the seafloor. During the October 2017 survey, these deep seawater properties became apparent as a signature of the buoyant effluent plume when they were juxtaposed against the ambient seawater characteristics in the mid and upper water column.

As described above, the legacies of entrainment anomalies can be particularly long-lived, remaining apparent within the water column well after completion of the initial dilution process. Anomalies, such as those captured on the north northeastern limit of the survey area during the shallow tow, provide useful tracers of the diffuse effluent plume during and after the completion of the initial dilution process. However, such anomalies are irrelevant to the receiving-water compliance assessment because the permit restricts attention to water-quality changes caused solely by the presence of wastewater constituents rather than by a simple relocation of ambient seawater.

Outfall Performance

The efficacy of the outfall can be evaluated through a comparison of dilution levels measured at the time of the October 2017 survey, and dilutions anticipated from modeling studies that were codified in the discharge permit through limits imposed on effluent constituents. Specifically, the critical initial dilution applicable to the MBCSD outfall was conservatively estimated to be 133:1 (Tetra Tech 1992). That is, dispersion modeling estimated that, at the conclusion of the minimum expected initial mixing, 133 parts of ambient seawater would have mixed with each part of wastewater.

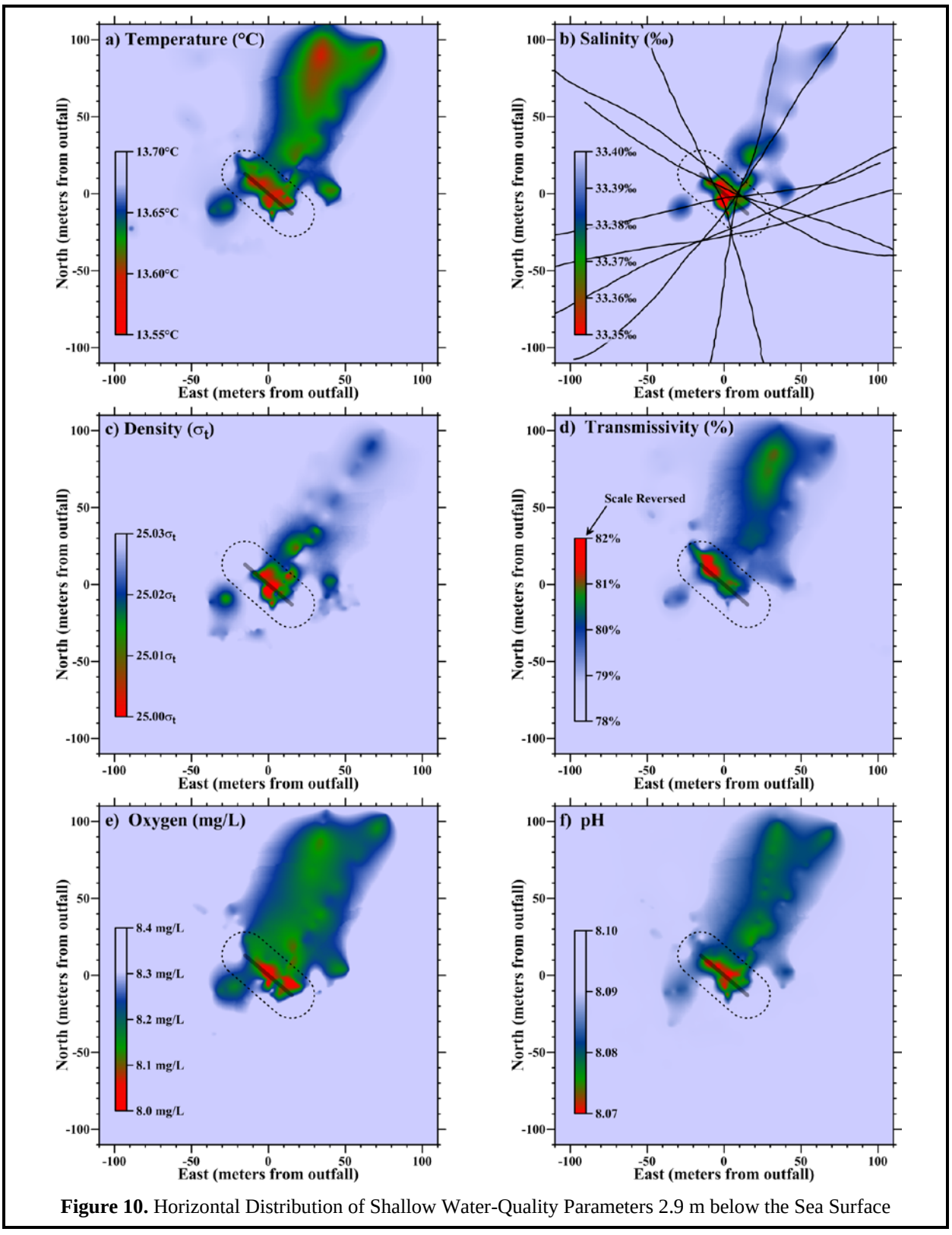

Figure 10. Horizontal Distribution of Shallow Water-Quality Parameters 2.9 m below the Sea Surface

The 133:1 dilution estimate was based on worst-case modeling under highly stratified conditions, where trapping of the plume below a strong thermocline would curtail the additional buoyant mixing normally experienced during the plume's ascent through the entire water column. Additionally, the modeling assumed quiescent oceanic flow conditions, thereby restricting initial mixing processes to the ZID. Under those conditions, the modeling predicted that a 133:1 dilution would be achieved after the plume rose only 9 m from the seafloor, whereupon it would become trapped, ceasing to ascend farther in the water column. At that point, the plume would spread laterally with dilution occurring at a much-reduced rate. A 9-m ascent at the MBCSD outfall translates into a trapping depth that is 6.2 m below the sea surface. As described below, however, the lowest dilution levels observed during the October 2017 survey were much higher than the 133:1 predicted by the modeling, even though they were measured within the ZID, at greater depth, and well before the completion of the initial dilution process.

The conservative nature of the critical initial dilution determined from the modeling is an important consideration because it was used to specify permit limitations on chemical concentrations within wastewater discharged from the treatment plant. These end-of-pipe effluent limitations were back calculated from the receiving-water objectives in the COP (SWRCB 2005) using the projected 133-fold dilution determined from the modeling. Application of a higher critical dilution would relax the stringent end-of-pipe effluent limitations thought necessary to meet COP objectives after initial dilution is complete.

End-of-pipe limitations on contaminant concentrations within discharged wastewater were based on the definition of dilution (Fischer et al. 1979). From the mass-balance of a conservative tracer, the concentration of a particular chemical constituent within effluent before discharge (C_e) can be determined from Equation 1.

$$C_e \equiv C_o + D\left(C_o - C_s\right) \qquad \text{Equation 1}$$

where: C_e = the concentration of a constituent in the effluent,
C_o = the concentration of the constituent in the ocean after dilution by D (i.e., the COP receiving-water objective),
D = the dilution expressed as the volumetric ratio of seawater mixed with effluent, and
C_s = the background concentration of the constituent in ambient seawater.

By rearranging Equation 1, the actual dilution achieved by the outfall can be determined from measured seawater anomalies. This measured dilution can then be compared with the critical dilution factor determined from modeling. Salinity is an especially useful tracer because it directly reflects the magnitude of ongoing dilution. The regions of slightly reduced salinity apparent directly over the outfall in both tow-survey maps (Figures 9b and 10b), and in the vertical profiles measured at five of stations (green shading in Figure 8abcde) were induced by the presence of dilute wastewater. These salinity anomalies document mixing processes within the effluent plume shortly after discharge, and as it rose through the water column and spread laterally.

The amplitudes of these salinity anomalies quantify the magnitude of wastewater dilution at the various stages of the initial mixing process. By rearranging Equation 1, the dilution ratio (D) can be computed from the salinity anomaly ($A = C_o - C_s$) as:

$$D \equiv \frac{(C_e - C_o)}{(C_o - C_s)} \propto -A^{-1} \qquad \text{Equation 2}$$

The salinity concentration within MBCSD effluent (C_e)[22] is small compared to that of the receiving seawater and, after dilution by more than 133 fold, the salinity of the effluent-seawater mixture is close to ambient salinity. Consequently, to a close approximation, dilution levels are inversely proportional to the amplitude of the salinity anomaly. Thus, a lower effluent dilution at a given location within the effluent plume is directly mirrored by a larger reduction in the measured salinity relative to that of the surrounding seawater.

Among the 10,665 CTD measurements collected during the October 2017 survey, the greatest reduction in salinity (-0.115‰) was recorded during the sixth transect of the mid-depth tow survey when a salinity of 33.449‰ was encountered only 1.3 m from the middle of the diffuser structure at a depth of 8.6 m (red shading in Figure 9b). From Equation 2, this salinity anomaly corresponds to a dilution of 280 fold (small patch of red centered within the ZID in Figure 11).

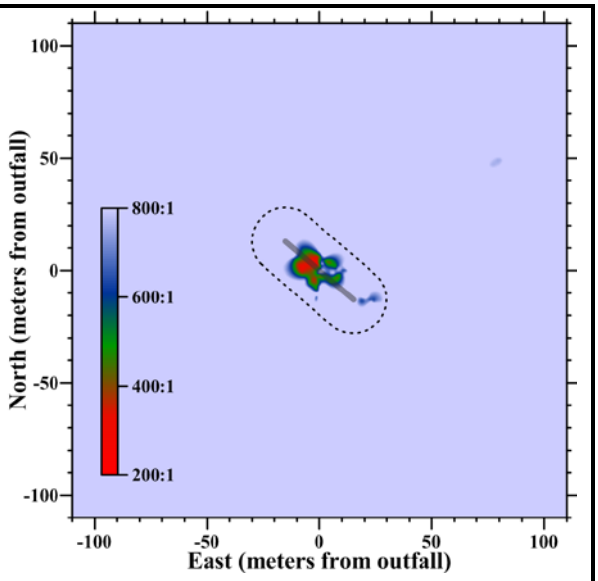

Figure 11. Mid-Depth Plume Dilution Computed from Salinity Anomalies in Figure 9b

The plume continued to mix as ascended rapidly toward the sea surface and began to spread laterally. Because of its rapid rise, only a slightly higher dilution of 281:1 was encountered within the core of the plume during the fourth transect of the shallow tow (bright red shading in Figure 12). However, the shallow tow also captured the plume's lateral spread directly beneath the sea surface, as well as its transport toward the north-northeast. As it spread beyond the ZID boundary, subsurface dilution levels increased rapidly, exceeding 380-fold along the ZID boundary (green shading along the dashed line northeast of the center of the diffuser structure). By the time the plume reached Station RW3, where the plume's salinity reduction was still plainly evident within the upper 5 m of the water column (green shading in Figure 8c), dilution levels exceeded 410-fold. The initial dilution process was nearing completion at that point and only slightly higher dilution levels were observed within the upper reaches of the water column at the other stations.

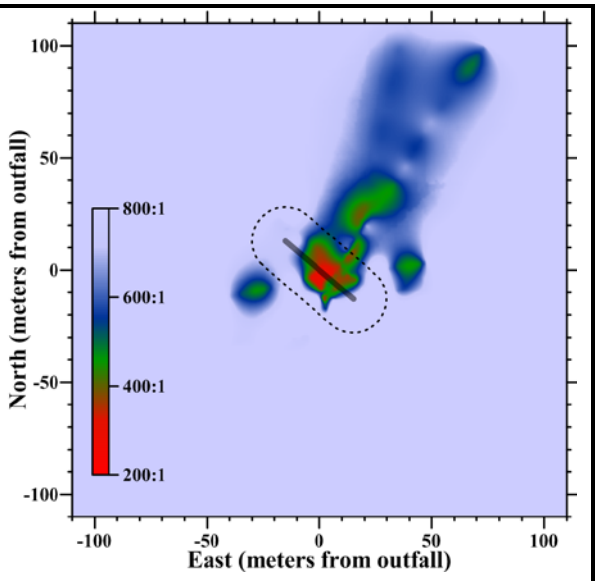

Figure 12. Shallow Plume Dilution Computed from Salinity Anomalies in Figure 10b

[22] Wastewater samples have an average salinity of 0.995‰.

Overall, these dilution measurements demonstrate that, during the October 2017 survey, the outfall was performing better than designed and was rapidly entraining seawater shortly after discharge. This resulted in dilution levels exceeding 280 fold well before the initial dilution process was complete. These minimum measured dilutions were double the 133:1 dilution predicted by the worst-case modeling study, even though they were measured at a depth 2.7 m below the model's 6.2-m trapping depth and were located directly over the diffuser structure rather than along the ZID boundary. Upon completion of the initial dilution process, measured dilutions were more than triple the model's 133:1 critical initial dilution that was used to establish end-of-pipe permit limitations on contaminant concentrations within wastewater discharged from the MBCSD treatment plant. This demonstrates that, during the October 2017 survey, the COP receiving-water objectives were being easily met by the limits on chemical concentrations within discharged wastewater that are promulgated by the NPDES discharge permit issued to the MBCSD.

COMPLIANCE

This section evaluates compliance with the water-quality limitations listed in the NPDES permit (Table 6). The limits themselves are based on criteria in the COP, the Central Coast Basin Plan, and other state and federal policies that were designed to protect marine life and beneficial uses of ocean waters. Because the limits only pertain to changes in water properties that are caused by the presence of wastewater constituents beyond the ZID, instrumental measurements undergo a series of screening procedures prior to numeric comparison with the permit thresholds. Specifically, the quantitative analyses described in this section focus on water-property excursions caused by the presence of wastewater constituents beyond the ZID, whose amplitudes can be reliably discerned against the backdrop of ambient fluctuations. A detailed understanding of ambient seawater properties, and their natural variability within the region surrounding the outfall, is therefore an integral part of the compliance evaluation presented in this section.

Table 6. Permit Provisions Addressed by the Offshore Receiving-Water Surveys

Limit #	Limit
P1	Floating particles or oil and grease to be visible on the ocean surface
P2	Aesthetically undesirable discoloration of the ocean surface
P3	Temperature of the receiving water to adversely affect beneficial uses
P4	Significant reduction in the transmittance of natural light at any point outside the ZID
P5	The DO concentration outside the zone of initial dilution to fall below 5.0 mg/L or to be depressed more than 10% from that which occurs naturally
P6	The pH outside the zone of initial dilution to be depressed below 7.0, raised above 8.3, or changed more than 0.2 units from that which occurs naturally

The results of the analyses performed on the October 2017 data demonstrate that the MBCSD discharge complied with the NPDES discharge permit. Moreover, although observations within the ZID are not subject to compliance evaluations, they met the prescribed limits because actual dilution levels routinely exceeded the conservative design specifications assumed in the discharge permit. Thus, the quantitative evaluation described in this section documents an outfall and treatment process that was performing at a high level during the October 2017 survey.

Permit Provisions

The offshore receiving-water surveys are designed to assess compliance with objectives dealing with undesirable alterations to six physical and chemical characteristics of seawater. Specifically, the permit states that wastewater constituents within the discharge shall not cause the limits listed in Table 6 to be exceeded.

The first two receiving-water limits, P1 and P2, rely on qualitative visual observations for compliance evaluation. Compliance was demonstrated during the October 2017 survey through visual inspection of the sea surface that documented an absence of floating wastewater materials, oil, grease, and discoloration of the sea surface.

Compliance with the remaining four receiving-water limitations was quantitatively evaluated through a comparison between instrumental measurements and numerical limits listed in the NPDES permit. For example, in P5 and P6, the fixed numeric limits on absolute values of DO (>5 mg/L) and pH (7.0 to 8.3) can be directly compared with field measurements within the dilute wastewater plume beyond the ZID. However, both P5 and P6 also contain narrative limits, which originate within the COP, and define unacceptable water-quality impacts in terms of "*significant*" excursions beyond those that occur "*naturally*." Quantitative evaluation of these limits requires a further comparison of field measurements with numerical thresholds that reflect the natural variation in temperature, transmissivity, DO, and pH within the receiving waters surrounding the outfall.

As described in prior sections, natural variation in seawater properties can result from a variety of oceanographic processes. These processes establish the range in ambient seawater properties caused by natural spatial variation within the survey region at a given time (e.g., vertical stratification), and by temporal variations caused by seasonal and interannual influences (e.g., El Niño and La Niña). Of particular interest are upwelling and downwelling processes that not only determine average properties at a given time, but also the degree of water-column stratification, or spatial variability, present during any given survey.

Screening of Measurements

Accurately evaluating whether any of the 10,665 CTD measurements collected during the October 2017 survey exceeded a permit limit can be a complicated process. For example, although apparently significant excursions in an individual seawater property may be related to the presence of wastewater constituents, they may also result from instrumental errors, natural processes, entrainment of ambient bottom water in the rising effluent plume, statistical uncertainty, ongoing initial mixing within and beyond the ZID, or other anthropogenic influences (e.g., dredging discharges or oil spills).

Because of this complexity, measurements were first screened to determine whether numerical limits on individual seawater properties even apply (Table 7). The screening procedure sequentially applies three questions to restrict attention to: 1) the oceanic area where permit provisions pertain; 2) changes due to the presence of wastewater constituents; and 3) changes large enough to be reliably detected against the backdrop of natural variation. The measurements that remain after completing the screening process can then be compared with Basin-Plan numerical limits and COP allowances.

The subsection following this one provides additional lines-of-evidence that demonstrate compliance with numerical permit limits independent of the screening process. The rationale for identifying observations suitable for further compliance analysis is presented in the following descriptions of the three screening steps.

Table 7. Receiving-Water Measurements Screened for Compliance Evaluation

Topic Addressed	Screening Question	Answer No	Answer Yes[23]	*Parameter*
Location	1. Was the measurement collected beyond the 15.2-m ZID boundary where modeling assumes that initial dilution is complete?	*1,557*	*9,108*	All
Wastewater Constituents	2. Did the beyond-ZID measurement coincide with a quantifiable salinity anomaly (≤550:1 dilution level) indicating the presence of detectable wastewater constituents?	*9,060*	*48*	All
Natural Variation	3. Did seawater properties associated with the wastewater measurements depart significantly from the expected range in ambient seawater properties at the time of the survey?	*48*	*0*	Temperature
		48	*0*	Transmissivity
		48	*0*	DO
		48	*0*	pH

1. Measurement Location: The COP states that compliance with its receiving-water objectives "*shall be determined from samples collected at stations representative of the area within the waste field where initial dilution is completed.*" Initial dilution includes the mixing that occurs from the turbulence associated with both the ejection jet, and the buoyant plume's subsequent ascent through the water column.

Although currents often transport the plume well beyond the ZID before the initial dilution process is complete, the COP states that dilution estimates shall be based on "*the assumption that no currents, of sufficient strength to influence the initial dilution process, flow across the discharge structure.*" Because of this, the regulatory mixing distance, which is equal to the 15.2-m water depth of the discharge, provides a conservative boundary to screen receiving-water data for subsequent compliance evaluation. Application of this initial screening question to the October 2017 dataset eliminated 1,557 of the original 10,665 receiving-water observations from further consideration because they were collected within the ZID (Table 7, Question 1). The remaining 9,108 observations were carried forward in the screening analysis.

2. Presence of Wastewater Constituents: The MBCSD discharge permit restricts application of the numerical receiving-water limits to excursions caused by the presence of wastewater constituents. This confines the compliance analysis to changes caused "*as the result of the discharge of waste*," as specified in the COP, rather than anomalies that arise from the upward movement of ambient seawater entrained within the buoyant effluent plume. Analyses conducted on quarterly receiving-water surveys over the last decade have demonstrated that the direct influence of dilute wastewater is almost never observed in any seawater property other than salinity, except very close (<1 m) to a diffuser port and within its ejection jet.

In fact, negative salinity anomalies are the only consistent indicator of the presence of wastewater constituents within receiving waters. Wastewater salinity is negligible compared to that of the receiving seawater, so the presence of a distinct salinity minimum provides *de facto* evidence of the presence of wastewater constituents. Because of the large contrast between the nearly fresh wastewater and the salty receiving water, salinity provides a powerful tracer of dilute wastewater that is unrivaled by other seawater properties. Other properties do not exhibit such a large contrast and, as such, their wastewater signatures dissipate rapidly upon discharge with very little mixing. Wastewater's lack of salinity, however, provides a definitive tracer that allows the presence of effluent constituents to be identified even

[23] Number of remaining CTD observations of potential compliance interest based on sequential application of each successive screening question

after dilution many times greater than the 133-fold critical initial dilution assumed in the discharge permit.

As described in the previous section, wastewater-induced reductions in salinity can be used to determine the amount of dilution achieved by initial mixing. Based on statistical analyses of the natural variability in salinity readings measured near the outfall over a five-year period between 2004 and 2008, the smallest reduction in salinity that can be reliability detected within receiving waters is 0.062‰. This represents a dilution level of 542 fold in Equation 2. Salinity reductions that are smaller than 0.062‰ cannot be reliably discerned against the backdrop of natural variation, and would not result in discernible changes in other seawater properties. Eliminating those measurements from further evaluation restricts attention to excursions in temperature, light transmittance, DO, and pH that are potentially related to the presence of wastewater constituents.

As discussed previously, the greatest salinity reductions observed during the October 2017 survey were recorded directly over the outfall during the mid-depth and shallow tow surveys. Although only a moderate oceanic current prevailed at the time of the survey, portions of the surfacing plume were carried well beyond the ZID before the initial dilution process was complete. As a result, a number of quantifiable salinity reductions were measured well outside the ZID boundary. Even though some of these 48 salinity anomalies were clearly measured prior to completion of the initial dilution process, they were outside the ZID and reliably associated with the presence of wastewater constituents (Table 7). The remaining 9,060 salinity measurements collected beyond the ZID during the October 2017 survey did not have salinity reductions that were larger than the 0.062‰ plume-detection threshold, and therefore corresponded to dilutions greater than 550:1.

3. Natural Variation: An integral part of the compliance analysis is determining whether a particular anomalous measurement resulted from the presence of wastewater constituents, or whether it simply became apparent because ambient seawater was relocated (upward) by the plume. If the measurement does not significantly depart from the natural range in ambient seawater properties at the time of the survey, then it is inappropriate to ascribe the departure to the presence of wastewater constituents. Thus, quantifying the natural variability around the outfall at the time of the survey is necessary for determining whether a particular observation warrants comparison with the numeric permit limits.

A statistical analysis of receiving-water data collected around the outfall was used to establish the range in natural conditions surrounding the outfall (first three data columns of Table 8 on the following page). These ambient-variability ranges were used to identify significant departures from natural conditions that could be indicative of adverse discharge-related effects on water quality. The same five-year database used to establish the within-survey salinity variation discussed previously, was also used to establish one-sided 95% confidence bounds on transmissivity (-10.2%), temperature (+0.82°C), DO (-1.38 mg/L), and pH (± 0.094). These were combined with 95^{th} percentiles determined from the October 2017 ambient seawater data, to establish time-specific natural-variability thresholds in a manner analogous to COP Appendix VI. The percentiles were determined from October-2017 vertical profile data collected largely at Station RW6, and excluded all measurements potentially affected by the discharge at other stations.

Temperature, transmissivity, pH, and DO concentrations associated with the 48 remaining measurements of potential compliance interest were all well within their respective ranges of natural variability (Table 7, Question 3). As such, the screening process unequivocally eliminated all of the measurements collected during the October 2017 survey from further consideration in the compliance analysis. In fact, all of the documented excursions in these properties were the result of physical processes unrelated to the presence of wastewater constituents, namely, entrainment of near-bottom seawater within the rising effluent plume.

Table 8. Compliance Thresholds

Water Quality Property	95% Confidence Bound[24]	95th Percentile[25,26]	Natural Variability Threshold[27]	COP Allowance[28]	Basin Plan Limit[29]	Extremum[30]
Temperature (ºC)	0.82	13.77	>14.59	>16.79	—	≤13.86
Transmissivity (%)	-10.2	74.3	<64.1	—	—	≥73.2
DO (mg/L)	-1.38	7.54	<6.16	<5.55	<5.00	≥7.40
pH (minimum)	-0.094	8.063	<7.968	<7.768	<7.000	≥8.048
pH (maximum)	0.094	8.123	>8.218	>8.418	>8.300	≤8.128

As discussed previously, anomalies in seawater properties clearly delineated the plume, but those entrainment-generated excursions were not caused by the presence of wastewater constituents. During periods when the water column is even slightly stratified, ambient seawater properties near the seafloor differ from those within the rest of the water column, and their juxtaposition within the rising effluent plume appears as lateral anomalies within the upper water column. Regardless, if the presence of wastewater particulates had contributed to the observed decreases in DO, pH and transmissivity within the upper water column, their influence would still have been well within the natural range of the ambient seawater properties at the time of the survey. Consequently, their influence on water quality would not be considered environmentally significant.

Other Lines of Evidence

Several additional lines of evidence further support the conclusion that all the CTD measurements collected during the October 2017 survey complied with the quantitative permit limits P3 through P6 in Table 6. In combination, these lines of evidence provide the "best explanation" of the origin and significance of individual measurements using abductive inference (Suter 2007). This process, which has been used to implement sediment-quality guidelines for California estuaries (SWRCB 2009), emphasizes a pattern of reasoning that accounts for both discrepancies and concurrences among multiple lines of evidence. A best explanation approach serves to limit the uncertainty associated with each individual CTD measurement, and to provide a more robust compliance assessment. Together, these lines of

[24] The one-sided confidence bound measures the ability to reliably determine ambient seawater properties within surveys as a whole. They were determined from an analysis of the variability in ambient water-quality data collected during 20 quarterly surveys conducted between 2004 and 2008. Although water-quality observations potentially affected by the presence of wastewater constituents were excluded from the analysis, more than 9,200 remaining observations for each of the six seawater properties accurately quantified the inherent uncertainty in defining the range in natural conditions.

[25] The COP (Appendix I, Page 27, SWRCB 2005) defines a "*significant*" difference as "*a statistically significant difference in the means of two distributions of sampling results at the 95% confidence level*." Accordingly, COP effluent analyses (Step 9 in Appendix VI, Page 42, Ibid.) are based "*the one-sided, upper 95% confidence bound for the 95th percentile*."

[26] The 95th-percentile quantified natural variability in seawater properties during the September 2017 survey itself, and was determined from vertical-profiles data unaffected by the discharge.

[27] Thresholds represent limits on wastewater-induced changes to receiving-water properties that significantly exceed natural conditions as specified in the discharge permit and COP. They are determined from the sum of columns to the left and are specific to the September 2017 survey. They do not include the COP allowances specified in the column to the right.

[28] The discharge permit, in accordance with the COP, allows excursions in seawater properties that depart from natural conditions by specified amounts. DO cannot be "*depressed more than 10% from that which occurs naturally*," and pH cannot be "*changed more than 0.2 units from that which occurs naturally.*" The California Thermal Plan is incorporated into the COP by reference, and restricts temperature increases to less than 2.2ºC.

[29] Permit limits P5 and P6 (Table 6) include specific numerical values promulgated in the RWQCB Basin Plan (1994) in addition to changes relative to natural conditions specified in the COP. The Basin Plan upper-bound pH objective for ocean waters is 8.5, but a more-stringent upper-bound objective of 8.3, which applies to individual beneficial uses, was implemented in the MBCSD discharge permit.

[30] Maximum or minimum value measured during the October survey, regardless of location within or beyond the ZID

evidence significantly strengthen the conclusion that the discharge fully complied with the permit at the time of the October 2017 survey.

Natural Variability within and beyond the ZID: Although the permit limits only apply to changes in DO, pH, temperature, and transmissivity beyond the ZID, examination of measurements acquired within the ZID frequently provides additional insight into the potential for adverse effects on water quality. However, among all the data collected during the October 2017 survey, salinity was the only seawater property that exhibited a perceptible difference from ambient conditions. Regardless of their association with the plume's effluent salinity signature or their proximity to the diffuser structure, none of the 10,665 temperature, DO, pH, and transmissivity observations exceeded the thresholds of natural variability specified in Table 8. This is apparent from a comparison between the extrema listed in the last data column in Table 8, and the corresponding natural-variability thresholds listed in third data column. For example, ambient seawater temperatures are expected to range as high as 14.59ºC, but the highest measured temperature was 13.86ºC. Similarly, natural excursions in transmissivity are expected to range as low as 64.1%, while the lowest measured transmissivity was 73.2%.

COP Allowances: The COP does not require that wastewater-induced changes remain within the ranges in natural variation listed in the third data column of Table 8, even though these ranges were conservatively used in the data screening process described in previous subsections. Consideration of these COP allowances for receiving-water limits provides an additional safety factor in the compliance evaluation of thermal, DO, and pH excursions.

For pH, the COP and the discharge permit allow changes up to 0.2 pH units from natural conditions, bringing the minimum allowed pH down to 7.768 for the October 2017 survey (fourth data column of Table 8). This limiting value is significantly less than the lowest pH measurement of 8.048 recorded during the October 2017 survey.[31] Similarly, the lowest DO concentration measured during the survey (7.40 mg/L) was well above the lower bound in expected natural variability (6.16 mg/L) and even more so for the less-stringent 10% compliance threshold promulgated by the COP (5.55 mg/L).

Limited Ambient Light Penetration: Although there are no explicit numerical objectives for discharge-related reductions in transmissivity, a numerical limit can be established from the COP requirement that the discharge not result in significant reductions in the transmission of natural light (P4 in Table 6). Because the COP does not specify an allowance beyond natural conditions, the 64.1% threshold on ambient transmissivity variations listed in third data column of Table 8 can be interpreted to constitute a numerical limit.

However, the COP objective for light penetration only applies to a limited subset of the transmissivity measurements. Because little natural light is present beneath the euphotic zone, which extends to twice the Secchi depth, the limit on transmissivity reductions during the October 2017 survey only applies to measurements recorded above 6 m (twice the shallowest Secchi depth listed in Table 4). This immediately eliminates 48% of the transmissivity measurements from further compliance consideration, even though they were included in the screening analysis. Specifically, even if the discharge of wastewater particulates had caused transmissivity measurements collected below the euphotic zone to drop below the numeric compliance threshold, it would not have been of regulatory concern because the penetration of ambient light would not have been affected. This includes measurements collected shortly after discharge near a diffuser port, or those within a naturally turbid boundary layer immediately above the seafloor, because virtually no natural light was present near the seafloor during the October 2017 survey.

[31] Compliance with COP maximum pH allowance (8.418) is irrelevant because effluent on the day of the survey had a pH of 7.3, which is much lower than the lowest pH measured within the receiving seawater (8.048). Consequently, the presence of effluent constituents could not have induced an increase in pH within receiving waters.

Insignificant Thermal Impact: As with transmissivity, there are no explicit numerical objectives for discharge-related increases in temperature. Nevertheless, a numerical limit can be established for thermal excursions that is based on the requirement that they not adversely affect beneficial uses (P3 in Table 6). Although the COP remains silent regarding allowable temperature changes, it incorporates the California Thermal Plan requirements by reference (COP Introduction §C.3). The Thermal Plan (SWRCB 1972) restricts temperature increases caused by new discharges to coastal water to be less than 2.2°C (4°F). As with DO and pH, a quantitative permit limit on temperature increases can be established by combining the Thermal Plan allowance with the natural variability threshold listed in the third data column of Table 8. Accordingly, increases in temperature caused by the discharge of warm wastewater during the October 2017 survey could be deemed to adversely affect beneficial uses if they exceeded 16.79°C (fourth data column of Table 8). However, none of the 10,665 CTD measurements collected during the survey exceeded 13.86°C (last column in Table 8). As a result, all the measurements remained well within the natural variability thermal threshold (14.79°C), and provided a much larger safety factor for compliance with the numerical limit derived from the Thermal Plan (16.79°C). In reality, temperatures measured within the rising effluent plume were uniformly below that of the surrounding seawater because cooler seawater near the seafloor had been entrained in the plume shortly after discharge. Consequently, any potential thermal impact resulting from the discharge of warm wastewater was almost immediately eliminated upon discharge because the effluent entrained large volumes of much colder seawater near the seafloor.

Directional Offset: Analysis of the directional offset of CTD measurements is useful because wastewater and receiving-seawater properties depart from one another in several predictable ways. Specifically, upon discharge, wastewater is fresher, warmer, more turbid, and less dense than the ambient receiving waters of Estero Bay. As such, the introduction of wastewater constituents will reduce the salinity, density, and transmissivity of the receiving seawater (negative offset), while temperature will be increased (positive offset). Therefore, the reduced temperatures observed in conjunction with the effluent plume during the tow surveys (Figures 9a and 10a) could not have been generated by the presence of warmer wastewater constituents. Instead, they were produced because the plume entrained cooler bottom water shortly after discharge. Similarly, the increased transmissivity observed within the discharge plume during the shallow tow (Figure 10d) could not have been generated by an unacceptably high particulate load within wastewater. In both cases, the directional offsets were opposite of receiving-water impacts expected from the presence of wastewater constituents.

Insignificant Wastewater Particulate Loads: Another independent line of evidence demonstrates that the discharge of wastewater particulates could not have contributed materially to turbidity within the dilute effluent plume, even before completion of the initial mixing process. The effluent suspended-solids concentration measured onshore at the time of the survey was 31 mg/L. After dilution by at least 280 fold, the effluent suspended-solids concentration would have the reduced ambient transmissivity by no more than 0.8%.

Similarly, the MBCSD discharge could not have contributed materially to the observed DO fluctuations. The MBCSD treatment process routinely removes 80% or more of the organic material, as demonstrated by the 38-mg/L BOD measured within the plant's effluent on the day after the survey. That small amount of BOD would have induced a DO depression of no more than 0.022 mg/L after dilution (MRS 2002). In fact, in the absence of a tangible BOD influence, wastewater discharge would actually be expected to increase DO within subsurface receiving waters, rather than decrease it. This is because effluent is oxygenated by recent contact with the atmosphere during the treatment process, whereas receiving waters at depth are typically depleted in DO due to the long absence of atmospheric equilibration within the deep offshore watermass.

Excursions remained within the fixed Basin-Plan Limits: Permit provisions P5 and P6 (Table 6) combine receiving-water objectives from both the COP and the Basin Plan with regard to DO and pH limits. As described previously, the COP requires that DO concentrations outside the ZID not be depressed more than 10% from that which occurs naturally, and restricts pH measurements to those within 0.2 units of that which occurs naturally. In contrast, the Basin-Plan's fixed numerical limits do not provide specific guidance as to how they might change in response to widespread changes in oceanographic conditions unrelated to the discharge. Specifically, the fixed numerical limits restrict DO concentrations outside the ZID to no less than 5 mg/L (P5 in Table 6), and pH levels to the 7.0-to-8.3 range (P6). As such, the fixed Basin-Plan limit on DO is less restrictive than the 5.55 mg/L minimum allowable DO concentration established for the October 2017 survey under COP objectives. Consequently, all of the DO measurements also easily complied with the Basin-Plan limit on DO reductions. Similarly, the minimum allowable pH (7.0) specified in the Basin Plan was less restrictive than the COP limit (7.786) specified for the October 2017 Survey, so all the pH observations again complied with both regulations.

CONCLUSIONS

The quantitative screening analysis demonstrated that all measurements recorded during the October 2017 survey complied with the receiving-water limitations specified in the NPDES discharge permit. This conclusion was further strengthened by other lines of evidence supporting compliance with the discharge permit. Specifically, although discharge-related changes in seawater properties were observed during the October 2017 survey, the changes were either not of significant magnitude (i.e., they were within the natural range of variability that prevailed at the time of the survey), were measured within the boundary of the ZID where initial mixing is still expected to occur, or were not directly caused by the presence of wastewater constituents within the water column (i.e., were entrainment generated).

Early in the initial mixing process, effluent was being diluted to levels in excess of 280-fold, which is double the critical dilution levels predicted by design modeling after completion of the mixing process. As the plume spread along the sea surface near the completion of initial mixing, dilution levels exceeded 400-fold. All of the measured dilution levels far exceed levels that were predicted by modeling and that were incorporated in the discharge permit as conservative limits on contaminant concentrations within effluent prior to discharge. Lastly, all of the auxiliary observations collected during the October 2017 survey demonstrated that the discharge complied with the narrative receiving-water limits in the discharge permit and the COP. Together; these observations demonstrate that the treatment process, diffuser structure, and the outfall continue to surpass design expectations.

REFERENCES

Davis, R.E., J.E. Dufour, G.J. Parks, and M.R. Perkins. 1982. Two Inexpensive Current-Following Drifters. Scripps Institution of Oceanography, University of California, San Diego, La Jolla, California. SIO Reference No. 82-28. December 1982.

Fischer, H.B., E.J. List, R.C.Y. Koh, J. Imberger, and N.H. Brooks. 1979. Mixing in Inland and Coastal Waters. New York: Academic Press, 482 p.

Kuehl, S.A., C.A. Nittrouer, M.A. Allison, L. Ercilio, C. Faria, D.A. Dukat, J.M. Jaeger, T.D. Pacioni, A.G. Figueiredo, and E.C. Underkoffler 1996. Sediment deposition, accumulation, and seabed dynamics in an energetic fine-grained coastal environment. *Continental Shelf Research*, 16: 787-816.

Marine Research Specialists (MRS). 1998. City of Morro Bay and Cayucos Sanitary District, Offshore Monitoring and Reporting Program, Semiannual Benthic Sampling Report, April 1998 Survey. Prepared for the City of Morro Bay, CA. July 1998.

Marine Research Specialists (MRS). 2002. City of Morro Bay and Cayucos Sanitary District, Supplement to the 2002 Renewal Application For Ocean Discharge Under NPDES Permit No. Prepared for the City of Morro Bay and Cayucos Sanitary District, Morro Bay, CA. July 2002.

Marine Research Specialists (MRS). 2011. City of Morro Bay and Cayucos Sanitary District, Offshore Monitoring and Reporting Program, 2010 Annual Report. Prepared for the City of Morro Bay, California. March 2011.

Marine Research Specialists (MRS). 2012. City of Morro Bay and Cayucos Sanitary District, Offshore Monitoring and Reporting Program, 2011 Annual Report. Prepared for the City of Morro Bay, California. March 2012.

Marine Research Specialists (MRS). 2013. City of Morro Bay and Cayucos Sanitary District, Offshore Monitoring and Reporting Program, 2012 Annual Report. Prepared for the City of Morro Bay, California. March 2013.

Marine Research Specialists (MRS). 2014. City of Morro Bay and Cayucos Sanitary District, Offshore Monitoring and Reporting Program, 2013 Annual Report. Prepared for the City of Morro Bay, California. March 2014.

National Academy of Sciences. 1993. Managing Wastewater in Coastal Urban Areas. National Research Council Committee on Wastewater Management for Coastal Urban Areas, Water Science and Technology Board, Commission on Engineering and Technical Systems. 477 pp.

Regional Water Quality Control Board (RWQCB) - Central Coast Region. 1994. Water Quality Control Plan (Basin Plan) Central Coast Region. Available from the RWQCB at 81 Higuera Street, Suite 200, San Luis Obispo, California. 148p. + Appendices.

Regional Water Quality Control Board (RWQCB) - Central Coast Region and the Environmental Protection Agency (USEPA) – Region IX. 1992a. Waste Discharge Requirements (Order No. 92-67) and Authorization to Discharge under the National Pollutant Discharge Elimination System (Permit No. CA0047881) for City of Morro Bay and Cayucos Sanitary District, San Luis Obispo County.

Regional Water Quality Control Board (RWQCB) - Central Coast Region and the Environmental Protection Agency (USEPA) – Region IX. 1992b. Monitoring and Reporting Program No. 92-67 for City of Morro Bay and Cayucos Sanitary District, San Luis Obispo County (Permit No. CA0047881).

Regional Water Quality Control Board (RWQCB) - Central Coast Region and the Environmental Protection Agency (USEPA) – Region IX. 1998a. Waste Discharge Requirements (Order No. 98-15) and National Pollutant Discharge Elimination System (Permit No. CA0047881) for City of Morro Bay and Cayucos Sanitary District, San Luis Obispo County. 11 December 1998.

Regional Water Quality Control Board (RWQCB) - Central Coast Region and the Environmental Protection Agency (USEPA) – Region IX. 1998b. Monitoring and Reporting Program No. 98-15 for City of Morro Bay and Cayucos Sanitary District, San Luis Obispo County. 11 December 1998.

Regional Water Quality Control Board (RWQCB) - Central Coast Region and the Environmental Protection Agency (EPA) – Region IX. 2009. Waste Discharge Requirements (Order No. R2-2008-0065) and National Pollutant Discharge Elimination System (Permit No. CA0047881) for the Morro Bay and Cayucos Wastewater Treatment Plant Discharges to the Pacific Ocean, Morro Bay, San Luis Obispo County. Effective 1 March 2009.

Sea-Bird Electronics, Inc. (SBE) 1989. Calculation of M and B Coefficients for the Sea-Tech Transmissometer. Application Note No. 7, Revised September 1989.

Sea-Bird Electronics, Inc. (SBE) 1992. SBE 12/22/22/20 Dissolved Oxygen Sensor Calibration and Deployment. Application Note No. 12-1, rev B, Revised April 1992.

Southern California Bight Field Methods Committee (SCBFMC). 2002. Field Operation Manual for Marine Water-Column, Benthic, and Trawl monitoring in Southern California. Technical Report 259. Southern California Coastal Water Research Project. Westminster, CA. March 2002.

State Water Resources Control Board (SWRCB). 1972. Water Quality Control Plan for Control of Temperature in the Coastal and Interstate Waters and Enclosed Bays and Estuaries of California. Revises and supersedes the policy adopted by the State Board on January 7, 1971, and revised October 13, 1971, and June 5, 1972. California Division of Water Quality, Water Quality Planning Unit.

State Water Resources Control Board (SWRCB). 2005. Water Quality Control Plan, Ocean Waters of California, California Ocean Plan. California Environmental Protection Agency. Effective February 14, 2006.

State Water Resources Control Board (SWRCB). 2009. Water Quality Control Plan for Enclosed Bays and Estuaries – Part 1 Sediment Quality. California Environmental Protection Agency. Effective August 22, 2009. sed_qlty_part1.pdf [Accessed 02/26/10].

Suter II, Glenn, W. 2007. Ecological risk assessment, 2nd edition. U. S. Environmental Protection Agency, Cincinnati, Ohio. CRC.

Tetra Tech. 1992. Technical Review City of Morro Bay, CA Section 201(h) Application for Modification of Secondary Treatment Requirements for a Discharge into Marine Waters. Prepared for the U.S. Environmental Protection Agency, Region IX, San Francisco, CA by Tetra Tech, Inc., Lafayette, CA. February 1992.